



Di Gregorio, F., Trajkovic, J., Roperti, C., Marcantoni, E., Di Luzio, P., Avenanti, A., Thut, G. and Romei, V. (2022) Tuning alpha rhythms to shape conscious visual perception. *Current Biology*, 32(5), 988-998.e6. (doi: [10.1016/j.cub.2022.01.003](https://doi.org/10.1016/j.cub.2022.01.003)).

This is the Author Accepted Manuscript.

There may be differences between this version and the published version. You are advised to consult the publisher's version if you wish to cite from it.

<http://eprints.gla.ac.uk/265262/>

Deposited on: 18 February 2022

Enlighten – Research publications by members of the University of Glasgow
<http://eprints.gla.ac.uk>

Tuning alpha rhythms to shape conscious visual perception

Francesco Di Gregorio^{1*}, Jelena Trajkovic^{2*}, Cristina Roperti², Eleonora Marcantoni², Paolo Di Luzio², Alessio Avenanti^{2,3}, Gregor Thut⁴, Vincenzo Romei^{2,5}

¹ UO Medicina riabilitativa e neuroriabilitazione, Azienda Unità Sanitaria Locale, via Castiglione 29, 40139, Bologna, Italy;

² Centro studi e ricerche in Neuroscienze Cognitive, Dipartimento di Psicologia, Alma Mater Studiorum – Università di Bologna, Campus di Cesena, via Pavese 50, 47521, Cesena, Italy;

³ Centro de Investigación en Neuropsicología y Neurociencias Cognitivas, Universidad Católica del Maule, Av San Miguel, 346000, Talca, Chile;

⁴ Centre for Cognitive Neuroimaging, School of Psychology and Neuroscience, University of Glasgow, 56-64 Hillhead Street, G12 8QB, Glasgow, UK;

⁵ IRCCS Fondazione Santa Lucia, Via Ardeatina, 306/354, 00179, Roma, Italy.

*Equally contributed

Corresponding author and Lead Contact: mail to vincenzo.romei@unibo.it (VR)
Centro studi e ricerche in Neuroscienze Cognitive, Dipartimento di Psicologia, Alma Mater Studiorum – Università di Bologna, Campus di Cesena, 47521 Cesena, Italy
Twitter Handle: @VincenzoRomei

Summary

It is commonly held that what we see and what we believe we see are overlapping phenomena. However, dissociations between sensory events and their subjective interpretation occur in the general population and in clinical disorders, raising the question as to whether perceptual accuracy and its subjective interpretation represent mechanistically dissociable events. Here, we uncover the role that alpha oscillations play in shaping these two indices of human conscious experience. We used electroencephalography (EEG) to measure occipital alpha oscillations during a visual detection task, which were then entrained using rhythmic-TMS. We found that controlling pre-stimulus alpha-frequency by rhythmic-TMS modulated perceptual accuracy but not subjective confidence in it, while controlling post-stimulus (but not pre-stimulus) alpha-amplitude modulated how well subjective confidence judgments can distinguish between correct and incorrect decision, but not accuracy. These findings provide the first causal evidence of a double-dissociation between alpha-speed and -amplitude, linking alpha-frequency to spatio-temporal sampling resources, and alpha-amplitude to the internal, subjective representation and interpretation of sensory events.

Keywords: Conscious Perception, Alpha Oscillations, Alpha Amplitude, Alpha Frequency, Visual Perception, Confidence, Rhythmic Transcranial Magnetic Stimulation, Alpha Entrainment.

1 **Introduction**

2 The well-known axiom “Seeing is believing” implies that what we see and what
3 we *believe* we see are largely overlapping phenomena. However, there are many
4 examples of dissociations between sensory events and their subjective
5 interpretation, both in the general population (i.e. false memories^{1,2}) and in
6 subclinical^{3,4} and clinical psychiatric populations (e.g. schizophrenia⁵). A key
7 question, therefore, is whether perceptual accuracy and its subjective interpretation
8 represent mechanistically dissociable events of our conscious experience. And, if so,
9 what their neural underpinnings might be.

10 Alpha oscillations (range 7-13Hz) in the human brain may play an active role in
11 both sensory processing and conscious perception⁶⁻¹⁵. In particular, pre-stimulus
12 alpha-amplitude has been shown to account for a momentary level of cortical
13 excitability¹⁶ and to predict subjective confidence in response to visual stimuli¹⁷⁻¹⁹.
14 Specifically, higher levels of alpha-amplitude seem to account for reduced subjective
15 confidence and reduced proneness to reporting a visual percept (more conservative
16 decision criterion), without affecting the level of accuracy of the response²⁰. These
17 new insights into the role of alpha-amplitude in perception suggest that alpha-
18 amplitude might not primarily reflect perceptual accuracy, but rather a change in the
19 internal response criterion. However, this leaves open a fundamental question: what
20 are the oscillatory correlates of perceptual accuracy?

21 Recent reports have highlighted the relevance of alpha-frequency in perceptual
22 sampling, with faster alpha oscillations resulting in higher temporal resolution and
23 more accurate perceptual experience²¹⁻²⁷, potentially through an increased
24 accumulation of sensory evidence over time. Importantly, we hypothesize here that
25 this higher temporal resolution of visual sampling can successfully translate into

26 higher accuracy in general, by allocating more resources to the perceptually relevant
27 sensory dimension within the same amount of time.

28 Here, in a first experiment, we have used a visual detection task with spatially
29 lateralized stimuli and electroencephalography (EEG), to directly test the hypotheses
30 that (1) alpha-frequency accounts for objective accuracy (correct vs. erroneous
31 responses and d' measures²⁸), while (2) alpha-amplitude predicts subjective
32 confidence (low vs. high confidence responses) and/or (3) relates to meta-cognitive
33 abilities, i.e. how well subjective confidence judgments can distinguish between
34 correct and incorrect decisions (as indexed by meta- d' measures²⁹).

35 Crucially, in a second experiment, we used rhythmic Transcranial Magnetic
36 Stimulation (rhythmic-TMS) prior to stimulus onset around individual alpha-frequency
37 (IAF) to entrain pre-stimulus oscillatory activity in the alpha-band towards slower or
38 faster alpha-frequency or higher alpha-amplitudes, in order to influence individual
39 performance towards lower or higher accuracy or to impact individual subjective
40 confidence levels, respectively.

41 Finally, as stimulus processing has been shown to influence metacognitive
42 abilities³⁰⁻³², in a third experiment, we delivered rhythmic-TMS at each participant's
43 own IAF post-stimulus but prior to a subjective confidence prompt to test how
44 increases in post-stimulus alpha-amplitude can modulate their ability to distinguish
45 between correct and incorrect decisions, measured by means of meta- d' .

46

Results

47 A total of 92 participants took part in three experiments (Figure 1), designed to map
48 pre-stimulus alpha-frequency and alpha-amplitude on objective versus subjective

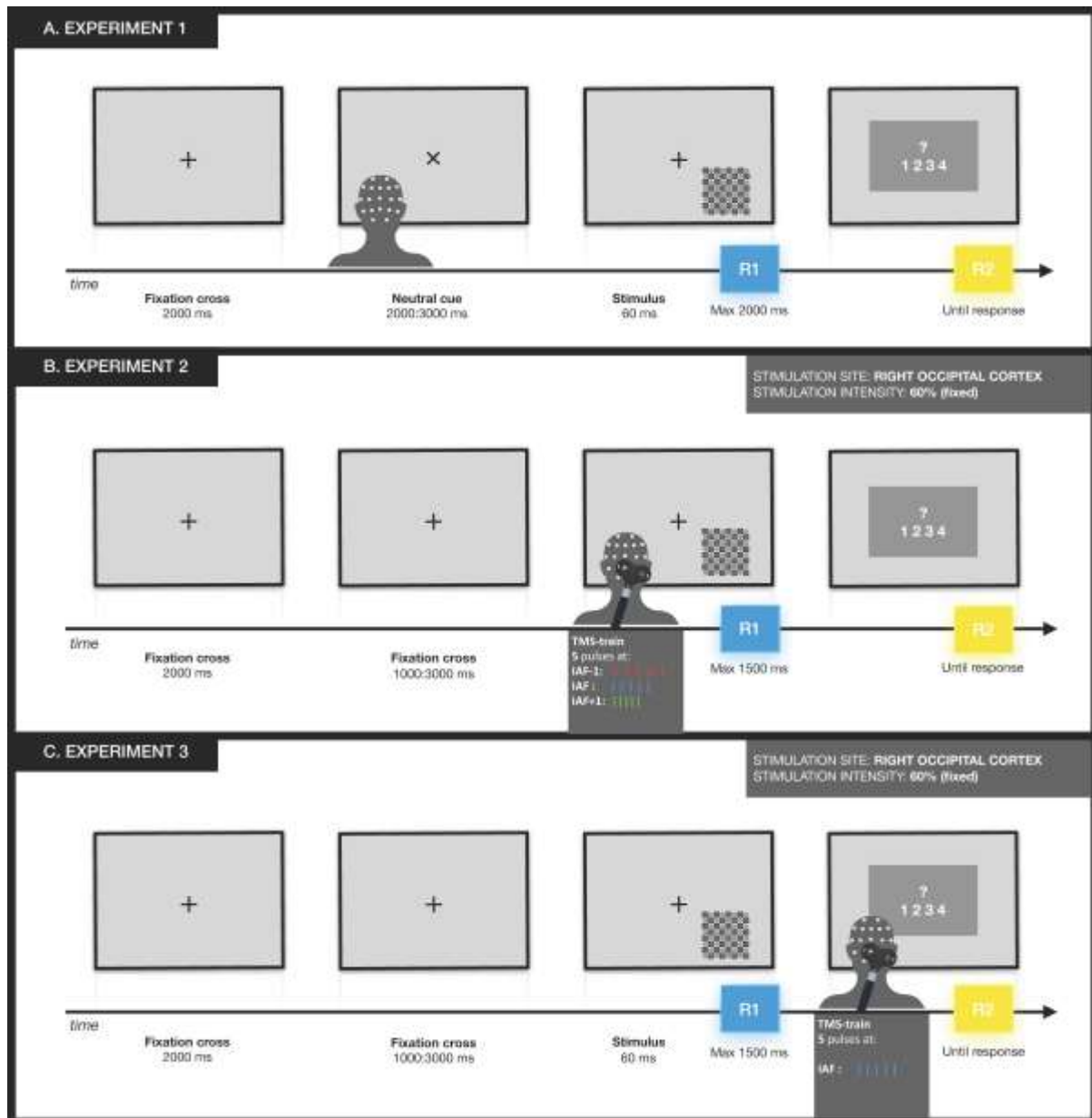
49 performance measures (EEG Experiment 1) and to test for their causative
50 relationships (TMS-EEG Experiments 2&3).

51

52 **Alpha-frequency and alpha-amplitude dissociate with respect to objective**
53 **accuracy, subjective confidence and metacognitive abilities**

54 In Experiment 1, twenty-four participants (12 women; mean age=23.2,
55 SE=2.61) performed a visual detection task (Figure 1A) in which lateralized stimuli
56 (8X8 checkerboards) were preceded by a spatially uninformative cue (an X),
57 indicating that a stimulus will be occurring in the lower left- or right-hemifield with
58 50% probability (chance level). Each black and white checkerboard was flashed for
59 60ms and could contain iso-luminant grey circles, the contrast of which was set for
60 each individual to their 50% perceptual threshold. Half of the trials were catch trials,
61 i.e. checkerboards without any grey circle embedded in them (see Methods for
62 details).

63 Participants were instructed to respond whenever they perceived grey circles
64 within the lateralized checkerboards. Following this primary task and about 1.5-2sec
65 post-stimulus, they were prompted to indicate on a scale of 1 to 4 how confident they
66 were of their percept, with 1 representing “no confidence at all”, 2, “little confidence”,
67 3 “moderate confidence” and 4 “high confidence” (see Figure 1A). EEG signals were
68 concurrently recorded from 64 electrodes while this task was performed (see
69 Methods).



70

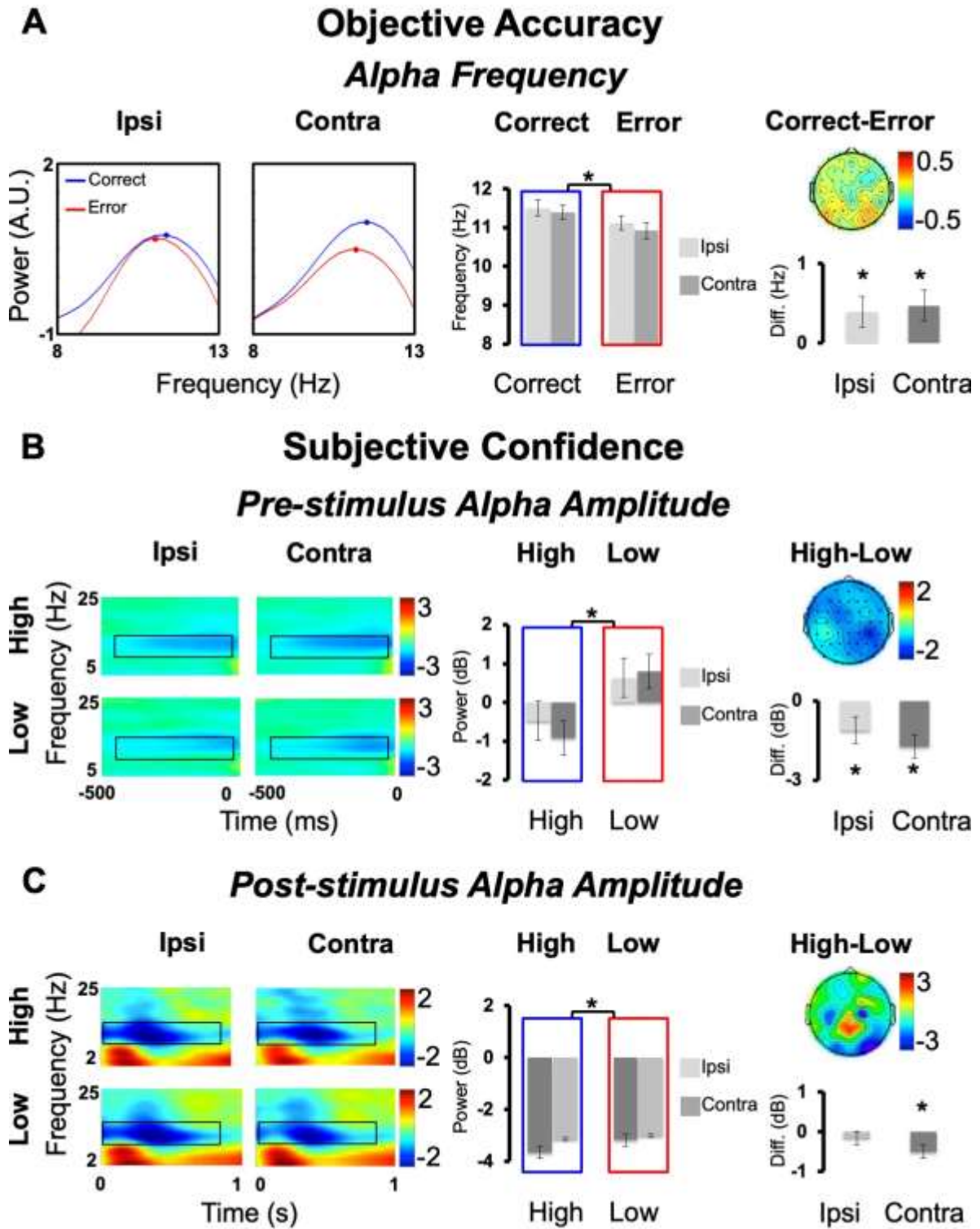
71 **Figure 1. Experimental design.** A. Experiment 1: EEG data were collected
 72 during a visual detection task. Each trial started with a fixation cross, after which
 73 stimuli could randomly appear in the lower left or right visual field. The primary task
 74 was to respond (R1) by pressing a space bar if the checkerboard contained grey
 75 grey circles. After this, participants rated their confidence in their first response (R2) on a
 76 Likert scale from 1 (no confidence at all) to 4 (high confidence). B. Experiment 2:
 77 Participants performed the same visual detection task as in Experiment 1 while
 78 undergoing concurrent EEG recording. In addition, 5 rhythmic-TMS pulses were
 79 administered before stimulus presentation. Participants were assigned to 3 different
 80 groups. For each group, rhythmic-TMS pulses were set at a certain alpha-frequency:
 81 individual alpha-frequency (IAF) group (blues bars), slower pace (IAF-1Hz) group
 82 (red bars), and faster pace (IAF+1Hz) group (green bars). C. Experiment 3:
 83 Participants performed the same visual detection task while undergoing EEG
 84 recordings, as in Experiments 1 and 2. However, rhythmic-TMS pulses were
 85 administered before the confidence prompt at each participant's individual alpha-
 86 frequency. ms=milliseconds.

87

88 *Pre-stimulus alpha-frequency and accuracy:* We looked at whether correct vs.
89 erroneous responses could be best explained by the frequency of alpha oscillations
90 prior to stimulus presentation, rather than by their amplitude. Our analysis of pre-
91 stimulus alpha-frequency (Figure 2A) showed a significant main effect of
92 ACCURACY (Correct vs. Errors) ($F(1,23)=18.2$, $p<.001$, $\eta_p^2=.442$). This result
93 suggests that individual pre-stimulus alpha-frequency can differentiate between
94 correct and erroneous responses, with faster alpha-frequency predicting correct
95 responses ($M=11.45\text{Hz}$, $SE=0.18\text{Hz}$) and slower alpha-frequency predicting errors
96 ($M=11.02\text{Hz}$, $SE=0.18\text{ Hz}$). Moreover, the effect of alpha-frequency was maximal
97 over the posterior electrodes (Figure 2A, map inset), involving left and right sites
98 equally, as no main effect of HEMISPHERE (ipsilateral vs. contralateral to the
99 presented stimulus) ($F(1,23)=1.34$, $p=.259$, $\eta_p^2=.06$), nor a significant interaction of
100 ACCURACYxHEMISPHERE ($F(1,23)=0.33$, $p=.571$, $\eta_p^2=.014$) were found.

101 We further tested whether pre-stimulus alpha-frequency can predict individual
102 performance across participants as assessed by d' , a sensitivity index that takes into
103 account both correct responses and false alarms, and thus – relative to the simple hit
104 rate measure – has the advantage of discounting any potential effect of response
105 bias, with higher values reflecting higher task accuracy²⁸. Using a median split
106 procedure for d' scores, we divided participants in two numerically equivalent groups
107 (high vs low d'). In line with our hypothesis, a between-groups analysis of alpha-
108 frequency show faster pre-stimulus alpha-frequency in the high d' group (11.55Hz,
109 $SE=0.22\text{Hz}$) compared to the low d' group (10.29Hz, $SE=0.66\text{Hz}$) by 1.26Hz:
110 $t(22)=1.832$, $p=.040$, $d=.374$ (one-tailed unpaired two-sample t-test).

111 By contrast, the analysis of both pre- and post-stimulus alpha-amplitude (see
 112 supplemental Figure S1B) showed no significant effects on ACCURACY (*all Fs*
 113 $(1,23) < 3.05$, *all ps* $> .094$, *all ηp^2* $< .117$), in line with recent reports that alpha-
 114 amplitude does not account for objective accuracy^{9,17,18,33}.



115

116 **Figure 2. Results Experiment 1: Alpha-frequency and -amplitude relate to**
117 **accuracy and confidence.** A. Objective Accuracy. Averaged *alpha-frequency* is
118 represented as the z-scored mean power ($10 \cdot \log_{10}[\mu\text{V}^2/\text{Hz}]$) spectrum in the cue-
119 stimulus time period for the contralateral and the ipsilateral electrodes and for
120 Correct and Error trials within the alpha-band. Bar graphs report correct and error
121 trials and the differences in correct/error responses. Topography represents the
122 difference in Correct-Error (electrodes are flipped to represent contralateral activity in
123 the right-hand side and ipsilateral activity in the left-hand side). Subjective
124 Confidence. Pre-stimulus alpha-amplitude (B) and post-stimulus alpha-amplitude (C)
125 are reported as time-frequency plots. For illustrative purposes we reported data from
126 a cluster of ipsi (P7,PO7,PO3,O1) and contralateral (P8,PO8,PO4,O2) electrodes
127 and for Low and High confident trials. Black boxes denote regions of statistical
128 analyses (alpha-band 7-13Hz). Bar graphs are reported for Low and High confident
129 trials and for the difference in High-Low. Topography represents the difference in
130 High-Low (electrodes are flipped to have contralateral activity in the right-hand side
131 and ipsilateral activity in the left-hand side). Two-tailed t-test statistical significance is
132 reported ($*p < .05$). Error bars represent standard error of the mean. A.U.=arbitrary
133 units; Diff=difference; μV =microvolt; Hz=Hertz; ms=milliseconds; dB=decibel.
134 See also Figure S1.
135

136 *Pre-stimulus alpha-amplitude and confidence:* We then tested whether pre-
137 stimulus alpha-amplitude, rather than alpha-frequency, could account for confidence
138 judgments^{17,18,6} (Figure 2B). We found a main effect of CONFIDENCE
139 ($F(1,23)=9.03$, $p=.006$, $\eta_p^2=.282$), with desynchronized alpha-amplitude in high
140 confidence trials (-0.699dB, SE=0.409dB) and synchronized alpha-amplitude in low
141 confidence trials (0.719dB, SE=0.251dB), suggesting that alpha-amplitude has a
142 significant impact on perceptual confidence. Moreover, topography (Figure 2B, map
143 inset) shows posterior alpha-amplitude modulations with an even distribution across
144 hemispheres, indicating no main effect of HEMISPHERE (ipsilateral vs. contralateral
145 to the presented stimulus) $F(1,23)=0.201$, $p=.658$, $\eta_p^2=.009$), nor a significant
146 interaction CONFIDENCExHEMISPHERE ($F(1,23)=1.323$, $p=.262$, $\eta_p^2=.054$).

147 For completeness, control analyses performed on pre-stimulus alpha-
148 frequency (see supplemental Figure S1A) showed no main effect of CONFIDENCE,
149 nor any interaction with HEMISPHERE (all $F_s(1,23) < 0.47$, $p_s > .501$, $\eta_p^2 < .021$).

150

151 *Post-stimulus alpha-amplitude, confidence and meta-d'*: Because following
152 stimulus presentation the initial choice on decisions and confidence continue to
153 evolve^{31,32}, we asked whether subjective confidence judgments are influenced by
154 post-perceptual processes. To this aim, we analysed alpha-amplitude in a time
155 window after stimulus presentation (0-900ms), corresponding to a post-stimulus time
156 period but before the confidence prompt (Figure 2C). The analysis of post-stimulus
157 alpha-amplitude revealed a main effect of CONFIDENCE ($F(1,23)=4.367$, $p=.048$;
158 $\eta_p^2=.16$), with more desynchronized alpha-amplitude in high confidence trials (-
159 3.41dB, SE=0.38dB) compared to low confidence trials (-3.08db, SE=0.34dB).
160 Moreover, the analyses showed a main effect of HEMISPHERE ($F(1,23)=5.358$;
161 $p=.03$; $\eta_p^2=.189$) and most importantly, an interaction
162 CONFIDENCExHEMISPHERE ($F(1,23)=4.347$, $p=.048$, $\eta_p^2=.159$), showing that
163 when looking at post-stimulus alpha-amplitude, the confidence effects are accounted
164 for by the contralateral (high confidence=-3.64dB, SE=0.396dB; low confidence=-
165 3.14dB, SE=0.347dB; $t(23)=2.747$, $p=.011$; $d=.586$) but not the ipsilateral
166 hemisphere (high confidence=-3.17dB, SE=0.387dB; low confidence=-3.01dB,
167 SE=0.349dB; $t(23)=0.906$, $p=.375$, $d=.193$). These findings suggest that post-
168 stimulus alpha-amplitude has a retinotopic distribution being modulated by the
169 stimulus position. Indeed, while the relationship between confidence levels and pre-
170 stimulus alpha-amplitude can be observed for both hemispheres, only contralateral
171 alpha-amplitude accounts for individual confidence levels after stimulus presentation.

172 We then tested whether post-stimulus alpha-amplitude could specifically
173 account for metacognitive abilities. In other words, we tested how well subjective
174 confidence judgments can distinguish between correct and incorrect decisions, by
175 means of meta-d', a measure that quantifies metacognitive performance and that

176 reflects the efficacy of confidence ratings to discriminate objectively correct from
177 erroneous responses²⁹. In a between-subject design, by using a median-split
178 procedure, we divided participants with high and low metacognitive abilities. We
179 found that post-stimulus alpha-amplitude in the high meta-d' group was significantly
180 more desynchronized (-4.66dB, SE=0.59dB) relative to the low meta-d' group (-
181 3.26dB, SE=0.39dB; one-tailed unpaired two-sample t-test: $t(22)=1.966$, $p=.031$;
182 $d=.567$), thus supporting the idea that post-stimulus alpha-amplitude can predict
183 metacognitive performance. Moreover, this role seems specific for post-stimulus
184 alpha-amplitude, as pre-stimulus changes of alpha-amplitude could not account for
185 between-subject differences in metacognition ($t(22)=0.929$, $p=.181$, $d=.189$), further
186 supporting this interpretation.

187

188 Overall, these EEG results implicate alpha-frequency in the level of objective
189 accuracy with higher alpha-frequency accounting for higher accuracy, but playing no
190 role in determining one's individual perceptual confidence. Conversely, alpha-
191 amplitude is implicated in perceptual decision confidence, but has no role to play in
192 objective accuracy. In sum, these results point to a functional dissociation of the two
193 oscillatory markers, alpha-frequency and alpha-amplitude, which appear to shape
194 sensory sampling and the subjective readout of this sampling, respectively.

195

196 **Entraining faster vs. slower pre-stimulus alpha oscillations selectively** 197 **shapes objective accuracy**

198 In Experiment 2, we tested for the causal involvement of alpha-frequency and
199 alpha-amplitude in objective accuracy vs. confidence by using rhythmic-TMS to
200 entrain alpha oscillations while participants performed the same visual task as in

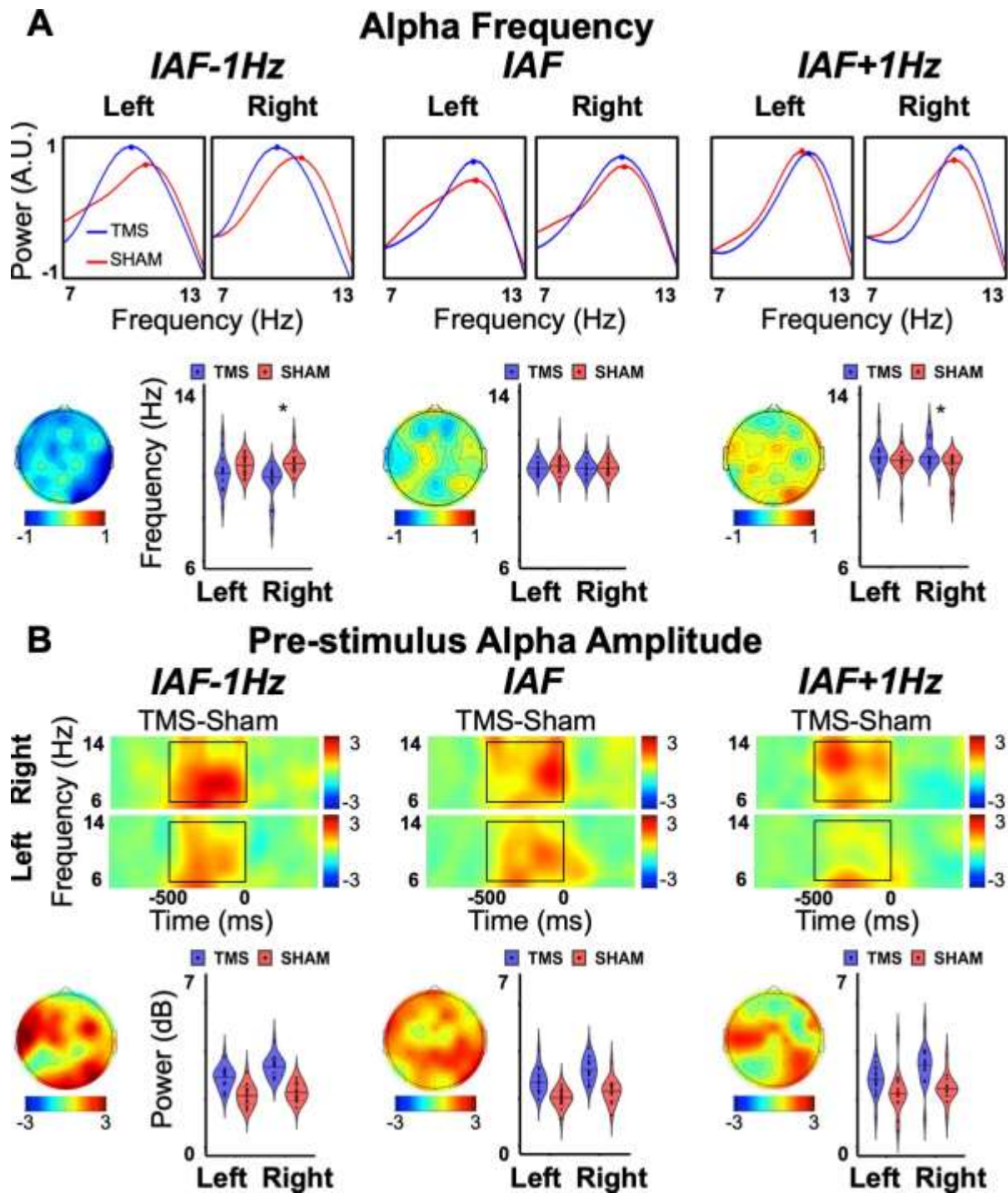
201 Experiment 1 (Figure 1B). In three different experimental groups (N=3x17
202 participants; 25 women; mean age=23.39, SE=0.36), we recorded EEG activity while
203 concurrently administering 5-pulse rhythmic-TMS trains of fixed-intensity (60% of the
204 maximum stimulator output)^{34,35} to the right occipital cortex (coil placement over O2)
205 prior to stimulus presentation. In the IAF±1Hz groups, rhythmic-TMS-frequency was
206 set at 1Hz faster/slower than the individual participant's alpha-frequency, which
207 should entrain their alpha oscillations towards a faster/slower pace^{21,22,36},
208 respectively. In the IAF group, the rhythmic-TMS frequency was aligned with the
209 participant's alpha-frequency. This has been shown to lead to enhanced alpha-
210 amplitude by entrainment^{37,38}, and should thus have an impact on confidence rather
211 than on accuracy. Together with active rhythmic-TMS, we employed sham
212 stimulation at a matching frequency for every participant in each group, to account
213 for any nonspecific effects of rhythmic-TMS.

214 Perceptual accuracy was quantified via d' score²⁸ (shown to be a more
215 sensitive measure relative to hit rates) while task confidence was estimated via
216 mean confidence and meta- d' . All measures were analysed across the two
217 hemifields (left vs. right), the two stimulation types (active rhythmic-TMS vs. sham),
218 and the three groups of participants (stimulated at IAF±1Hz and IAF).

219 We looked at the impact of rhythmic-TMS on EEG activity across the 3 groups
220 (Figure 3). As expected, pre-stimulus alpha-frequency was modulated differently in
221 active rhythmic-TMS versus sham stimulation across the experimental groups,
222 depending on the recording site (STIMULATIONxGROUPxHEMISPHERE
223 interaction: $F(2,48)=4.05$, $p=.024$, $\eta_p^2=.144$). Specifically, stimulating at the lower
224 alpha-frequency slowed down pre-stimulus alpha activity during active rhythmic-TMS
225 (M=9.74Hz, SE=0.20), relative to sham stimulation (M=10.66Hz, SE=0.20),

226 selectively at the (stimulated) right hemisphere ($t(16)=3.98$, $p=.001$, $d=.96$).
227 Conversely, stimulation at the higher alpha-frequency led to faster pre-stimulus alpha
228 activity during active rhythmic-TMS ($M=11.11\text{Hz}$, $SE=0.14$), relative to sham
229 stimulation ($M=10.43\text{Hz}$, $SE=0.31$), selectively at the stimulated site ($t(16)=2.19$,
230 $p=.043$, $d=.53$). Finally, stimulation at the exact alpha-frequency did not yield any
231 difference in the pre-stimulus alpha speed ($t(16)=0.13$, $p=.90$, $d=.03$). Moreover, we
232 found that rhythmic-TMS maximally entrained oscillatory activity exactly at the site of
233 stimulation (HEMISPHERE \times STIMULATION interaction: $F(1,48)=6.36$, $p=.015$,
234 $\eta_p^2=.117$), and at the entrained rhythm (see Figure 3A).

235 By contrast, the broadband alpha-amplitude (see Figure 3B) did not differ
236 significantly across the three groups during the entrainment protocol
237 (HEMISPHERE \times STIMULATION \times GROUP interaction: $F(2,48)=0.19$, $p=.830$,
238 $\eta_p^2=.008$). However, the entrainment effect on alpha-amplitude (quantified via the
239 difference between active rhythmic-TMS and sham stimulation) was largest at the
240 frequency of stimulation (FREQUENCY \times GROUP interaction: $F(4,96)=5.640$, $p<.001$,
241 $\eta_p^2=.19$, for details, see supplemental figure S2).



242

243

244

245

246

247

248

249

250

251

252

Figure 3. Results Experiment 2: rhythmic-TMS entrainment modulates EEG alpha-frequency and its amplitude. Results are shown for each group performing the task in Experiment 2 under different rhythmic-TMS alpha entrainment protocols (IAF \pm 1Hz, IAF). A. (Upper) Averaged Alpha-frequency is represented as the z-scored mean power ($10 \cdot \log_{10}[\mu\text{v}^2/\text{Hz}]$) spectrum during rhythmic-TMS in the pre-stimulus time period (-650 0) in the right (stimulated) hemisphere (electrode cluster: O2,PO4,PO8) and left (non-stimulated) hemisphere (electrode cluster: O1,PO3,PO7), for active rhythmic-TMS (TMS) and SHAM-control stimulation. (Lower) Violin plots report peak frequency during TMS and SHAM for each group (IAF \pm 1Hz, IAF) and for the left and right (stimulated) hemisphere. Data are

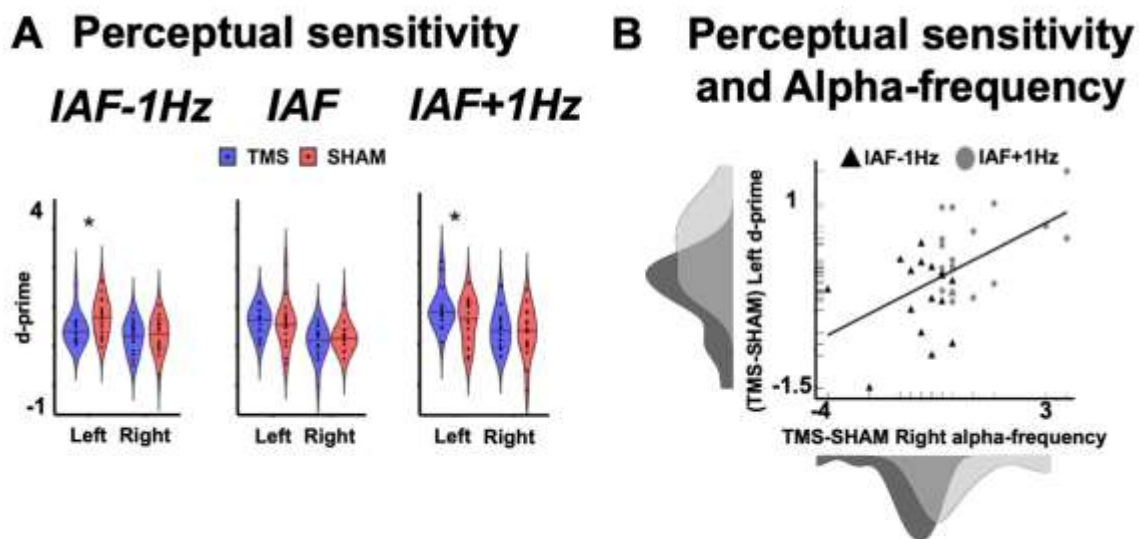
253 presented as median (full line) ± 1 quartile (dashed line). The topography image
254 represents the difference in alpha-frequency between TMS and SHAM stimulation.
255 B. (Upper) Pre-stimulus alpha-amplitude is presented as time-frequency plots for
256 each group (IAF \pm 1Hz, IAF) of the difference between TMS and SHAM stimulation in
257 the right (stimulated) hemisphere (electrode cluster: O2,PO4,PO8) and in the left
258 (non-stimulated) hemisphere (electrode cluster: O1,PO3,PO7). Black boxes denote
259 regions of statistical analyses (alpha-band 7-13Hz in the pre-stimulus period (-
260 500,0)). (Lower) Violin plots report alpha power during TMS and SHAM for each
261 group, and for the left and right (stimulated) hemisphere. Data are presented as
262 median (full line) ± 1 quartile (dashed line). Topography represents the difference in
263 alpha-amplitude between TMS and SHAM stimulation. Two-tailed t-test statistical
264 significance is reported (* $p < .05$). Error bars represent standard error of the mean.
265 A.U.=arbitrary units; Diff=difference; μ v=microvolt; Hz=Hertz; ms=milliseconds;
266 dB=decibel.
267

268 When examining the impact of entrainment on behavior (Figure 4A), we found
269 that speeding up or slowing down alpha oscillations had a direct impact on
270 performance (STIMULATION \times GROUP \times HEMIFIELD interaction ($F(1,48)=3.25$,
271 $p=.047$, $\eta p^2=.119$). Specifically, slowing-down pre-stimulus alpha-frequency led to
272 lower d' scores in the active rhythmic-TMS condition (relative to sham stimulation)
273 exclusively in the hemifield contralateral to stimulation ($t(16)=2.67$, $p=.017$, $d=.65$). In
274 contrast, speeding-up pre-stimulus alpha-frequency led to higher d' values during
275 active rhythmic-TMS (relative to sham stimulation), exclusively in the contralateral
276 hemifield ($t(16)=2.52$, $p=.023$, $d=.61$). Finally, entrainment at individual alpha-
277 frequencies did not yield differences in task accuracy, as predicted (all $t_s(16) < 1.19$,
278 all $p_s > .252$, all $d_s < .29$). We further tested whether the impact of rhythmic-TMS on
279 EEG oscillatory activity could account for the magnitude of the behavioral modulation
280 induced by the TMS protocol (Figure 4B). To do so, we examined the relationship
281 between sham-corrected performance and sham-corrected entrained frequency
282 across participants (IAF \pm 1Hz groups included). The results reveal that a significant
283 positive relationship exists between the TMS-induced change in oscillatory peak

284 frequency and performance gain ($R^2=0.29$, $p=.001$), further confirming a link
 285 between alpha-frequency and performance accuracy.

286 Our results thus far indicate that pre-stimulus alpha-frequency, but not alpha-
 287 amplitude, has a causative role in sampling sensory input, accounting for visual
 288 accuracy.

289



290

291 **Figure 4. Results Experiment 2: rhythmic-TMS entrainment causally links**
 292 **alpha speed to perceptual accuracy.** A. Perceptual sensitivity. Results are
 293 presented for three groups of participants (IAF \pm 1Hz and IAF stimulation protocol).
 294 Perceptual sensitivity is quantified in d' scores. Violin plots of d' are reported for
 295 rhythmic-TMS (TMS) and SHAM-control stimulation, and separately for the left and
 296 right hemifields. Data are presented as median (full line) \pm 1 quartile (dashed line). B.
 297 Perceptual sensitivity and alpha-frequency. Relationship between TMS-induced
 298 differences in alpha-frequency in the stimulated (right) hemisphere (computed as a
 299 difference in alpha-frequency between TMS and SHAM stimulation) and differences
 300 in accuracy in the opposite (left) hemifield (computed as a difference in d' score
 301 between TMS and SHAM stimulation), across the slower (IAF-1Hz group,
 302 represented as black triangles) and faster rhythmic-TMS groups (IAF+1Hz group,
 303 represented as grey circles). Density distributions of the two variables across the two
 304 groups are also presented along the corresponding axes. t-test statistical
 305 significance is reported (* $p<.05$).

306

307 **Alpha-amplitude dynamics shape subjective confidence and metacognition,**

308 **not accuracy**

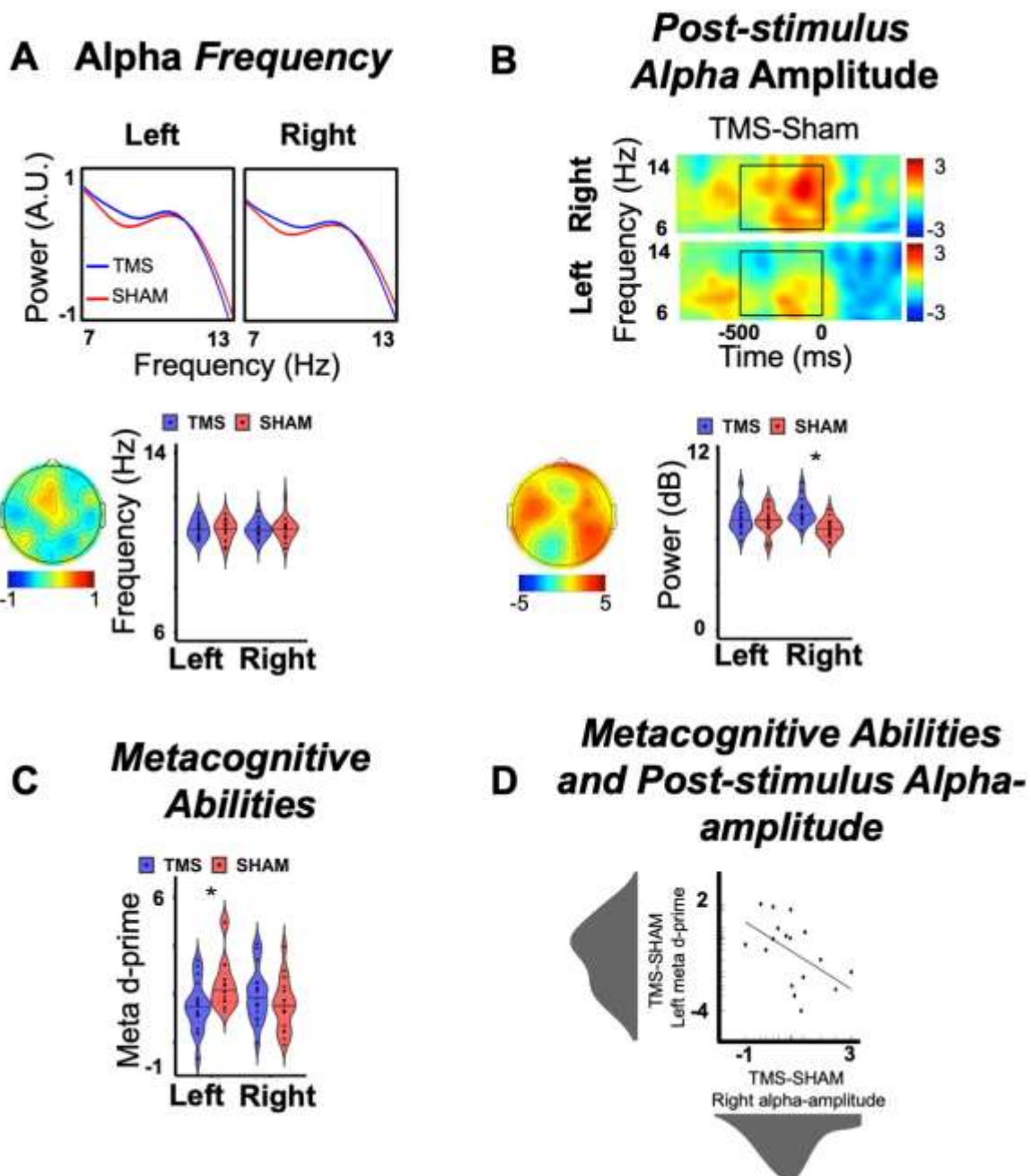
309 Another goal of Experiment 2 was to determine whether alpha-amplitude
310 dynamics causally shape subjective representation and interpretation of perceptual
311 performance. However, confidence levels and metacognitive abilities – as measured
312 via confidence mean and meta-d' scores²⁹ respectively – appeared not to be
313 affected across the three different stimulation protocols nor between the two
314 hemifields, as neither the main effects of GROUP, HEMIFIELD and STIMULATION,
315 nor their interactions, reached significance (all $F_s(2,48) < 2.72$, all $p_s > .076$, all
316 $\eta p^2 < .102$). The short-term nature of entrainment effects might explain these null
317 results, as they are limited to a few hundreds of milliseconds following
318 stimulation^{37,39,40}. This is long enough for pre-stimulus TMS entrainment to influence
319 the primary accuracy response, as this was collected immediately after stimulus
320 presentation. The secondary, higher decision confidence response, however, which
321 was associated with pre-stimulus EEG alpha-amplitude, was collected only 1.5-2 sec
322 post-stimulus (through the confidence prompt) and hence occurred >1 sec after
323 rhythmic-TMS offset (see Figure 1B), when entrainment effects might not be
324 sufficiently sustained anymore^{37,41}. Therefore, in order to further assess the causal
325 role of alpha-amplitude dynamics in perceptual awareness, and particularly in
326 metacognitive abilities, we ran a third follow-up experiment aimed at entraining post-
327 stimulus alpha-amplitude in seventeen participants (12 women; mean age=22.47,
328 SE=0.66). This group received 5-pulse rhythmic-TMS trains that were tailored to
329 their individual alpha-frequency with pulses applied just before the confidence
330 prompt, i.e. after stimulus presentation (see Figure 1C). The aim of this protocol was
331 to enhance alpha-amplitude by rhythmic-TMS without affecting alpha-speed.
332 Importantly, analysis of the alpha-amplitude in the post-stimulus period in
333 Experiment 1 justified the timing of this stimulation, as alpha-amplitude after stimulus

334 presentation (i.e. the time window of stimulation in Experiment 3) was related to
335 subjective confidence (with lower contralateral alpha-amplitude leading to high
336 confidence responses) and metacognitive abilities.

337 EEG analyses in Experiment 3 revealed a maximal entrainment effect in
338 broadband alpha-amplitude prior to the confidence prompt during active rhythmic-
339 TMS relative to sham stimulation at the stimulated site
340 (HEMISPHERE \times STIMULATION interaction: $F(1,16)=6.91$, $p=.002$, $\eta p^2=.302$).
341 Moreover, as expected, the rhythmic-TMS trains at IAF did not have any effect on
342 the alpha frequency measured prior to confidence judgment (all $F_s(1,16)< 0.19$, all
343 $p_s>.666$, all $\eta p^2<.012$) (Figure 5A, B). Crucially, this selective modulation of alpha-
344 amplitude right before confidence judgment allowed us to causally test the impact of
345 alpha-amplitude on metacognitive abilities vs. subjective confidence ratings. Our
346 results show clear effects on metacognition, as highlighted by distinct modulations of
347 meta- d' scores, between active rhythmic-TMS and sham stimulation, depending on
348 hemifield (HEMIFIELD \times STIMULATION interaction: $F(1,16)=4.73$, $p=.045$, $\eta p^2=.228$)
349 (Figure 5C). Specifically, higher alpha-amplitudes prior to the confidence prompt led
350 to lower meta- d' scores during active rhythmic-TMS vs. sham stimulation, exclusively
351 in the contralateral hemifield ($t(16)=2.74$, $p=.014$, $d=.66$). Importantly, these induced
352 changes in post-stimulus alpha-amplitude had a selective impact on metacognitive
353 abilities and not on confidence measures or on perceptual accuracy (all
354 $F_s(1,16)<.82$, all $p_s>.379$, all $\eta p^2<.049$), thus confirming the role of post-stimulus
355 alpha-amplitude in higher-level post-perceptual decision making.

356 Finally, we tested whether individual differences in TMS-induced post-stimulus
357 alpha-amplitude modulations could account for the level of metacognitive abilities. To
358 do so, we analyzed the relationship between sham-controlled TMS-induced alpha-

359 amplitude and sham-controlled meta-d' levels for stimuli presented in the
 360 contralateral hemifield. We found a significant inverse relationship, confirming that
 361 the higher the impact of rhythmic-TMS on alpha-amplitude, the lower the resulting
 362 level of metacognition of the individual response ($R^2=0.27$, $p=.032$; Figure 5D).
 363 These results strongly support a role of post-stimulus alpha-amplitude in selectively
 364 shaping our metacognitive abilities, with higher post-stimulus alpha-amplitude
 365 leading to lower metacognition.



366

367 **Figure 5. Results Experiment 3: rhythmic-TMS entrainment causally links**
368 **post-stimulus alpha-amplitude to metacognitive abilities.** A. (Upper) Averaged
369 Alpha-frequency is represented as the z-scored mean power ($10 \cdot \log_{10}[\mu\text{V}^2/\text{Hz}]$)
370 spectrum in a pre-confidence time period (850 1500) in the right (stimulated)
371 hemisphere (electrode cluster: O2,PO4,PO8) and in the left (non-stimulated)
372 hemisphere (electrode cluster: O1,PO3,PO7) for rhythmic-TMS and SHAM-control
373 stimulation. (Lower) Violin plots report peak frequency during TMS and SHAM,
374 separately for the left and right (stimulated) hemisphere. Data are presented as
375 median (full line) ± 1 quartile (dashed line); Topography represents the difference in
376 alpha-frequency between TMS and SHAM stimulation. B. (Upper) Post-stimulus
377 alpha-amplitude reported as a time-frequency plot of the difference between TMS
378 and SHAM stimulation in the right (stimulated) hemisphere (electrode cluster:
379 O2,PO4,PO8) and in the left (non-stimulated) hemisphere (electrode cluster:
380 O1,PO3,PO7). Black boxes denote regions of statistical analyses (alpha-band 7-
381 13Hz in the pre-confidence stimulation period (1000,1500)). (Lower) Violin plots
382 report alpha-power during TMS and SHAM stimulation, and separately for the left
383 and right (stimulated) hemisphere. Data are presented as median (full line) ± 1
384 quartile (dashed line). Topography represents the difference in alpha-amplitude
385 between TMS and SHAM stimulation. C. Metacognitive Abilities, quantified via meta-
386 d' scores. Violin plots of meta d' for TMS and SHAM-control stimulation, and
387 reported separately for the left and right hemifields. Data are presented as median
388 (full line) ± 1 quartile (dashed line). D. Metacognitive Abilities and Post-stimulus
389 Alpha-amplitude. Relationship between rhythmic-TMS-evoked differences in alpha-
390 amplitude in the stimulated (right) hemisphere (computed as a difference in alpha-
391 amplitude between TMS and SHAM stimulation) and differences in metacognition in
392 the opposite (left) hemisphere (computed as a difference in meta- d' score between
393 TMS and SHAM stimulation). Density distributions of the two variables are also
394 presented along the corresponding axes. Two-tailed t-test statistical significance is
395 reported ($*p < .05$). A.U.=arbitrary units; μV =microvolt; Hz=Hertz; ms=milliseconds;
396 dB=decibel.
397

398 **Discussion**

399 The oscillatory underpinnings of conscious perception have been the focus of
400 many studies, yet they remain largely unknown. A number of studies have previously
401 reported that pre-stimulus alpha oscillations over occipital sites might play a role in
402 human perceptual performance prediction^{e.g.16,42–45}, highlighting the potential
403 existence of a direct link between levels of alpha activity, cortical excitability and
404 perceptual sensitivity. Recent findings^{17,18,20,33,46} have, however, challenged these
405 past interpretations, and have highlighted the need to dissociate the processes that
406 shape perceptual sensitivity from those that shape the subjective interpretation of a

407 sensory event²⁸. Here, we disentangle the oscillatory dynamics of these two
408 processes and go beyond a correlative approach. By using an information-based
409 rhythmic-TMS protocol³⁶, we demonstrate that distinct markers of alpha activity have
410 a causal role in shaping our conscious perception, a role that goes beyond that of a
411 simple epiphenomenon. By directly manipulating alpha-frequency and -amplitude at
412 the site of stimulation^{47,48}, we were able to dissociate perceptual sensitivity from the
413 subjective representation and interpretation of a sensory event, thus demonstrating
414 their dualistic nature.

415 Our findings show that the speed of occipital alpha activity has a crucial and
416 selective role in modulating perceptual sensitivity. This adds to previous reports
417 showing that alpha cycles account for sampling sensory information into discrete
418 units/perceptual frames (initially proposed by⁴⁹ and reviewed in¹²). From this, one
419 might expect that higher frequency would translate in higher accuracy when
420 information can be sampled over many cycles. But why would this effect show even
421 when a sensibly short-lasting stimulus, certainly shorter than one alpha cycle, is
422 presented, as in our case? With our experimental design (60ms stimulus duration),
423 there is only one chance (sample) to capture the stimulus within an alpha cycle. And
424 what would this tell us about the underlying mechanism? To address this, we provide
425 here an exemplar account of the impact of frequency variations on sampling efficacy
426 for a 9Hz and 11Hz alpha oscillation. For these oscillations, cycles will range
427 between 110ms (for 9Hz IAF) and 90ms (for 11Hz IAF). However, processing
428 abilities will vary within the cycle, with a rapid fluctuation from a high to low
429 excitability phase (from alpha peak to trough)⁵⁰⁻⁵³. Hence, sampling is expected to
430 occur in one half of this cycle only, i.e. during ~55ms for 9Hz and ~45ms for 11Hz,
431 respectively. Our data suggest that this sampling is more effective with higher than

432 lower alpha frequencies, even with stimuli as short as 60ms, suggesting that
433 evidence accumulation already starts to differ within one sampling sweep across
434 variations of alpha-frequencies. This can be explained by enhanced processing
435 capacities for shorter than longer cycles, because with the shorter sampling phases
436 (~45ms), our short-lasting stimulus (60ms) is more likely to be fully comprehended in
437 one perceptual frame. For stimuli of longer durations (e.g. 1000ms), one would
438 expect repeated sampling sweeps to further add to this difference, as more full-
439 sample sweeps can be packed in 1sec at high than low frequencies (11 vs. 9
440 sweeps, for 11Hz vs 9Hz). In sum, here we claim that in line with existing
441 literature^{23,24,33} higher frequencies are expected to aid temporal resolution by
442 creating more sampling frames per second; but our data show that, at the same
443 time, in the context of our specific experiment, higher frequency also means that less
444 time is employed to create a single sampling frame, leading to higher processing
445 capacities.

446 Our EEG findings furthermore show an inverse relationship between levels of
447 alpha-amplitude and subjective confidence confirming previous findings¹⁷⁻¹⁹. Indeed,
448 pre-stimulus alpha-amplitude has been proposed to relate to internal decision-
449 making variables^{18,20}, rather than perceptual accuracy per se. Yet, our experimental
450 manipulation by rhythmic-TMS could not verify the existence of a causal link
451 between pre-stimulus alpha-amplitude and confidence. However, several studies
452 have concluded that our sense of confidence is also determined by processes that
453 occur after we make a choice, thus integrating sensory evidence and improving our
454 “metacognitive accuracy”, namely the extent to which our confidence is consistent
455 with our probability of being correct^{e.g.31,54,55}. Examining post-stimulus alpha-
456 amplitude, Experiments 1 and 3 demonstrate that after lateralized stimuli are

457 presented, perceptually relevant, post-stimulus alpha-amplitude become focused in
458 the hemisphere contralateral to stimulus presentation, with lower alpha-amplitude
459 leading to higher perceptual confidence. Moreover, these levels of post-stimulus
460 alpha desynchronization directly account for metacognitive abilities across
461 participants and can be causally manipulated by rhythmic-TMS. These latter results
462 suggest that post-stimulus alpha modulations may reflect the integration of
463 confidence judgment with the accumulated evidence after stimulus presentation to
464 update and adjust metacognitive decisions^{31,55,56}. Taken together, these results
465 speak in favor of a relevant role of alpha-amplitude in post-perceptual decision
466 making. Therefore, it might be possible that pre-stimulus alpha-amplitude dictates
467 the initial level of perceptual bias (effects observed for confidence bilaterally, but not
468 metacognitive effects), that subsequently integrates sensory evidence brought by the
469 stimulus itself (reflected in hemisphere-specific processes), resulting in post-
470 perceptual estimation of the performance.

471 While our experiments show that alpha-frequency and –amplitude, and hence
472 sensitivity and confidence, are dissociable entities, these processes likely work in
473 concert in more ecological situations to maximize the efficiency of our conscious
474 experience. We observed that the entrainment effects on oscillation and perception
475 showed corresponding topographic/retinotopic distributions, with perception being
476 exclusively modulated in the hemifield contralateral to the stimulated site, suggesting
477 that the oscillatory substrates of effective sampling and subjective confidence could
478 be oriented in space to optimize the allocation of attention resources. Therefore,
479 under controlled conditions (for example by presenting informative cues⁵⁷ or in
480 predictive contexts⁵² that are associated with spatial priors), one might expect the
481 spatially specific co-occurrence of alpha-frequency and -amplitude modulation that is

482 contralateral to the to-be-attended or expected location^{59,60}. Future research into the
483 inter-dependency of these two circuits may shed new light on different
484 neuropsychological phenomena. For example, the failure to integrate perceptual
485 processes and their subjective interpretation might lead to altered cognitive
486 experiences, such as confabulations or the formation of false representations and
487 memories, with relevant implications for clinical and forensic neuropsychology. The
488 failure to integrate perceptual processes and their subjective interpretation may also
489 lead to conscious departure from sensory events in acute schizophrenia patients⁶¹.

490 In conclusion, our results point to a functional dissociation between the
491 accuracy of what we see and our interpretation of it. We reveal that the sampling of
492 visual information and its subjective interpretation, which are strongly inter-
493 dependent in everyday life, are dissociable in terms of neural mechanisms in
494 oscillatory activity. Specifically, alpha-frequency and -amplitude reflect the activity of
495 these two independent mechanisms that serve complementary functions. Alpha-
496 frequency represents a spatial and temporal sampling mechanism^{27,62-64} that shapes
497 perceptual sensitivity. By contrast, alpha-amplitude dictates more liberal vs
498 conservative choices in confidence judgments, further modulated with incoming
499 sensory evidence, thus having post-perceptual effect on how these subjective
500 confidence judgments can distinguish between correct and incorrect decisions^{17,19}.
501 How these mechanisms interact to give rise to an integrated (or not) sense of our
502 perceptual environment, is yet to be addressed. However, we demonstrate that
503 these oscillatory processes can be selectively modulated by non-invasive
504 neurostimulation, offering a foundation to future translational neuroscience
505 approaches and clinical applications.

506

507 **Acknowledgments**

508 FDG is supported by the Ministero della Salute (SG-2018-12367527); AA is
509 supported by Fondazione del Monte di Bologna e Ravenna (339bis/2017), Bial
510 Foundation (347/18) and Ministero dell'Istruzione, dell'Università e della Ricerca
511 (2017N7WCLP); VR is supported by the Bial Foundation (204/18);

512

513 **Author contributions**

514 VR conceived the project; VR, FDG, JT, CR, AA, GT designed the experiment;
515 VR, FDG, EM, PDL, JT, CR, Implemented the experiment; JT, EM, PDL and CR
516 conducted the experiment; FDG and JT analysed data; FDG, JT and VR wrote the
517 first draft of the paper. VR, FDG, EM, PDL, JT, CR, AA GT contributed to the final
518 draft of the paper.

519

520 **Declaration of Interests**

521 The authors declare no competing interests.

522

523

524

525

526

527

528

529

530

531

532

533 **STAR Methods**

534 **Resource availability**

535 *Lead contact.* Further information and requests for resources and reagents should
536 be directed to and will be fulfilled by the Lead Contact, Vincenzo Romei
537 (vincenzo.romei@unibo.it).

538

539 *Materials availability.* See the Key resources table for information about resources.
540 This study did not generate new unique reagents.

541

542 *Data and code availability.* The datasets generated during this study have been
543 made publicly available through the Open Science Framework (<https://osf.io/e4bnj/>).
544 Any additional information required to reanalyse the data reported in this paper is
545 available from the lead contact upon request.

546

547 **Experimental model and subject details**

548 ***Experiment 1***

549 *Participants:* Twenty-four healthy volunteers (12 women, 12 men; mean age=
550 23.2, SE=2.61) with normal or corrected vision participated in Experiment 1. Sample
551 size was determined based on previous literature. Specifically, previous EEG studies
552 on the role of pre-stimulus alpha in conscious perception considered a sample size
553 between 10 and 26 participants^{18,33,65,66}. In addition, post-hoc power analysis (G-
554 power 3.1) revealed that, for all significant ANOVA effects in our study, values of
555 Power (1- β err prob) are >0.95. All participants were recruited at the Centre for
556 Studies and Research in Cognitive Neuroscience in Cesena, Italy. The study was

557 conducted in accordance with the Declaration of Helsinki. All participants gave
558 written informed consent to participate in the study, which was approved by the
559 bioethics committee of the University of Bologna.

560 ***Experiment 2***

561 *Participants.* Fifty-one healthy volunteers (25 females, 26 males; mean age \pm
562 SE = 23.39 \pm 0.36 years) took part in Experiment 2. Sample size was determined
563 based on previous literature. Specifically, previous TMS studies on oscillatory
564 entrainment considered a sample size between 7 and 17^{35,37,67–71}. In addition, post-
565 hoc power analysis (G-power 3.1) revealed that, for all significant ANOVA effects in
566 our study, values of Power (1- β err prob) are >0.95. All of the participants had
567 normal or corrected-to-normal vision and met TMS safety criteria by self-report. All
568 participants gave written informed consent before taking part in the study, which was
569 conducted in accordance with the Declaration of Helsinki and approved by the local
570 ethics committee. Here, subjects were randomly assigned to one of three groups,
571 with distinct stimulation protocols (see Methods details section): IAF-1Hz (group
572 1=mean age 22.64 \pm 0.52, nine females), IAF (group 2=mean age 23.88 \pm 0.52, eight
573 females) and IAF+1Hz (group 3=mean age 23.88 \pm 0.77, eight females), each
574 containing 17 participants.

575 ***Experiment 3***

576 *Participants.* Seventeen healthy new volunteers (12 women, 5 men; mean
577 age=22.47, SE=0.66) were recruited for Experiment 3.

578

579 **Method details**

580 ***Experiment 1***

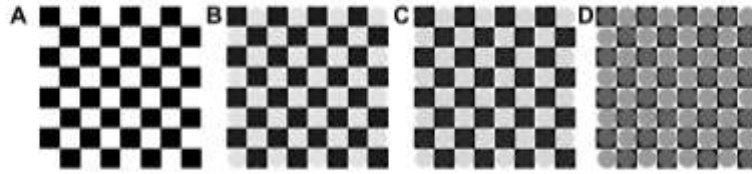
581 *Stimuli and task procedure.* Participants were comfortably seated in front of a
582 CRT monitor (100Hz refresh rate) at a viewing distance of 57cm. A PC running E-
583 Prime software (Psychology Software Tools, Inc., USA) controlled stimulus
584 presentation and responses registration. During the main experimental procedure
585 (main task), each trial consisted of a *primary visual detection task*, in which
586 participants responded to visual stimuli displayed on the computer screen, and a
587 *secondary confidence task*, in which participants rated the level of confidence in their
588 perception on a scale of 1 to 4, where 1=no confidence at all; 2=little confidence;
589 3=moderate confidence; and 4=high confidence. At the beginning of each trial, a
590 white fixation cross was displayed on a grey background. The fixation cross was
591 presented in the centre of the screen for 2000ms and subtended a visual angle of
592 0.8°. Afterwards, an X (visual angle 2°) was created by rotating the fixation cross by
593 45 degrees. The cue appeared for a variable time period (time jitter between 2000
594 and 3000ms), immediately followed by the primary task stimulus. The stimulus could
595 appear with equal probability on the right or left visual field. These stimuli were
596 presented at 4.1°/3.7° eccentricity (horizontal/vertical) in the lower part of the left
597 visual field (LVF) or right visual field (RVF) for 60ms. The primary task stimulus could
598 be either a catch stimulus (50% of trials) or a target stimulus (50% of trials). Catch
599 stimuli consisted of 8x8 black and white checkerboards (height=4cm; width=4cm.
600 visual angle=15.9°). Target stimuli consisted of the same checkerboard containing
601 iso-luminant grey circles, which contrasted the black and white parts of the
602 checkerboard. Participants were prompted to press the spacebar on the keyboard
603 with their right index finger whenever they detected the circles embedded in the
604 checkerboard. Primary response speed was not stressed over perceptual accuracy,
605 but a time limit of 2000ms was given. After this primary response, confidence ratings

606 were collected. The Italian version of the question: “How confident are you about
607 your percept?” was presented until participants rated their confidence. Confidence
608 was rated on a 4-points Likert scale, from “no confidence at all” to “high confidence”,
609 and was reported by pressing the corresponding number on the keyboard with the
610 left index finger. Notably, here the confidence rating reflects a participant’s level of
611 subjective certainty in having correctly perceived the stimulus⁷². After rating their
612 confidence, a new trial started with the presentation of a new fixation cross. The
613 main task consisted of 5 blocks with 60 trials per block (total trial number=300) and
614 lasted on average 90min.

615

616 *Titration session.* A titration session was run before the main experimental
617 session in order to set stimuli contrast ratios corresponding to each individual’s 50%
618 perceptual threshold. Iso-luminant circles of 8 different contrast ratios (RGB
619 contrasts on black/white background: 28/227, 32/223, 36/219, 40/215, 44/211,
620 48/207 and 100/155) were presented together with catch trials (checkerboards
621 without iso-luminant circles). Please note examples of stimuli of different contrasts:
622 A. Catch Stimulus B. Low Contrast Stimulus (RGB contrasts: 30/225) C. High
623 Contrast Stimulus (RGB contrasts:40/215) D. Maximum Contrast Stimulus (RGB
624 contrasts:100/155).

625 To account for individual biases among participants in their response to catch
626 trials, a false alarm rate was considered, together with target stimuli of different
627 contrast for the calculation of the sigmoid function. For each iso-luminant contrast,
628 individual performance was then entered to calculate the sigmoid function.



629

630 **Figure 6. Examples of stimuli of different contrasts. A. Catch Stimulus B.**
 631 **Low Contrast Stimulus (RGB contrasts: 30/225) C. High Contrast Stimulus (RGB**
 632 **contrasts:40/215) D. Maximum Contrast Stimulus (RGB contrasts:100/155)**
 633

634 Data were analyzed using the following formula to calculate the threshold value
 635 (y):

636

637
$$y = \frac{100}{1 + e^{-\frac{x-c}{d}}}$$

638

639 Where x is the contrast value, c is the inflection point of the curve and d is the
 640 slope of the sigmoid.

641 The corresponding inflection point was selected as the bias-adjusted threshold,
 642 which was used for stimulus presentation during the experiment. In Experiment 1,
 643 detection performance threshold during the main task (M=56.9%, SE=3.69%) was
 644 not statistically different from the bias-adjusted threshold (M=51.58%, SE=0.48%)
 645 calculated during the titration session, ($t(24)=1.68$, $p=.11$, $d=0.34$). Across
 646 participants, the selected luminance contrast ratios during the main task ranged
 647 between 20/235 and 50/205 RGB points (M=32/223, SE=12).

648

649 **Experiment 2**

650 Both Experiment 2 and Experiment 3 implemented a rhythmic-TMS
651 entrainment protocol with concurrent EEG recording. The timing of rhythmic-TMS
652 pulses differed between the two experiments.

653 *Stimuli and task procedure.* Stimuli and tasks in Experiment 2 were the same
654 as those described for Experiment 1, with the main difference being the active
655 manipulation of alpha activity via an entrainment protocol.

656 Entrainment of the intrinsic oscillatory alpha activity was achieved using
657 rhythmic transcranial magnetic stimulation (rhythmic-TMS). Specifically, pre-stimulus
658 alpha activity was fine-tuned relative to individual alpha-frequency using rhythmic
659 five-pulse TMS bursts in which the time lag between pulses was manipulated
660 depending on the group^{21,73}. In order to induce changes in the alpha-frequency cycle
661 length, rhythmic-TMS was applied at a slower or faster pace, relative to a
662 participant's individual alpha-frequency. To selectively modulate alpha-amplitude, the
663 frequency of the rhythmic-TMS pulse trains was matched to the intrinsic individual
664 alpha-frequency of the participant, thus enhancing the synchronization of neural
665 firing and phase alignment without influencing the speed of alpha activity. In this
666 way, rhythmic-TMS pulse trains could occur at three different frequencies: at the
667 individual alpha-frequency of the participant to manipulate pre-stimulus alpha-
668 amplitude (IAF group); at 1Hz lower than the individual alpha-frequency (IAF-1Hz
669 group) to slow-down pre-stimulus alpha-frequency; or at 1Hz higher than the
670 individual alpha-frequency (IAF+1Hz group) to speed-up pre-stimulus alpha-
671 frequency. In all groups, the last TMS-pulse coincided with the stimulus appearance.

672 Biphasic stimulation was applied using a Magstim Rapid Transcranial Magnetic
673 Stimulator via a 70mm figure-of-eight coil (Magstim Company, UK) of maximum field
674 strength ~1.55T. As systematic differences in visual cortex excitability do not seem

675 to be present between the hemispheres^{34,74–76}, TMS bursts were delivered only to
676 the right occipital site (at O2 electrode position), with the coil surface tangent to the
677 scalp, and the handle oriented perpendicular to the medial plane of the subjects
678 head (latero-medial current direction). Moreover, pulse intensity was kept fixed at
679 60% of the maximum stimulator output (MSO)^{34,77–79}, roughly corresponding to
680 previously reported phosphene thresholds^{80–84}. No subject reported to have
681 perceived phosphenes during the execution of the task. Within-subject sham control
682 stimulation was implemented in order to account for any non-specific rhythmic-TMS
683 effects. To do so, a modified coil was used that provided enough distance from the
684 scalp to ensure the absence of stimulation, while at the same time maintaining coil
685 position, as well as tactile and acoustic sensations. Each participant underwent three
686 consecutive rhythmic-TMS and sham blocks (resulting in a total of 900 active
687 rhythmic-TMS pulses), whereas rhythmic-TMS/sham stimulation block order was
688 randomized. Therefore, the experimental session consisted of 6 blocks with 60 trials
689 per block (total trial number=360) (see also Experiment 1), with short breaks
690 between the blocks (overall average task duration of 50 minutes). The rhythmic-TMS
691 design was in line with current safety guidelines⁸⁵.

692

693 *Titration session.* Titration was run as for Experiment 1. Additionally, in the
694 second experiment, during the titration session, individual alpha peak frequency
695 (defined as the maximum local power in the alpha-frequency range) was determined.
696 A total of six minutes resting-state EEG (three minutes with eye closed and three
697 minutes with eyes open, and with gaze on a fixation cross on the screen) was
698 recorded from 8 Ag/AgCl parieto-occipital electrodes (O1,P3,PO3,PO7; O2,P4,PO4,
699 PO8). Individual alpha-frequency peak was calculated from the power spectra of the

700 eyes open condition, applying a Fast Fourier Transformation. In line with Experiment
701 1 (showing a local alpha power maxima over O2) and previous studies, alpha-
702 frequency was calculated from the O2 electrode^{21,83}, over which rhythmic-TMS was
703 subsequently applied (see above). The identified individual alpha-frequency was
704 used to calibrate rhythmic-TMS frequency.

705

706 ***Experiment 3***

707 *Stimuli and task procedure.* The stimuli and task for Experiment 3 were the
708 same as those used for Experiment 2, the main difference being the timing of the
709 manipulation of alpha activity via an entrainment protocol.

710 Specifically, Experiment 3 aimed to selectively enhance post-stimulus alpha-
711 amplitude, prior to the confidence prompt. As such, only one entrainment protocol
712 was applied (i.e. stimulation at the individual alpha-frequency). While in Experiment
713 2, the final pulse of the rhythmic-TMS-train coincided with stimulus onset, in
714 Experiment 3, the final rhythmic-TMS pulse coincided with the onset of the
715 confidence prompt.

716 Stimulation site, coil orientation, stimulation intensity, control conditions and
717 number of pulses were the same as those used in Experiment 2.

718

719 *Titration session.* The titration session was conducted as in Experiment 2.

720

721 **Quantification and Statistical Analysis**

722 ***Experiment 1***

723 *Psychophysiological recording – paradigm and acquisition.* EEG data were
724 collected during the main task in Experiment 1 from 64 Ag/AgCl electrodes

725 (Fp1,Fp2,AF3,AF4,AF7,AF8,F1,F2,F3,F4,F7,F8,FC1,FC2,FC3,FC4,FC5,FC6,FT7,F
726 T8,C1,C2,C3,C4,C5,C6,T7,T8,CP1,CP2,CP3,CP4,CP5,CP6,TP7,TP8,P1,P2,P3,P4,
727 P5,P6,P7,P8,PO3,PO4,PO7,PO8,O1,O2,Fpz,AFz,Fz,FCz,Cz,CPz,Pz,POz,Oz) and
728 from the right mastoid with Brain Vision recorder software (Brain Products, Munich,
729 Germany). The left mastoid was used as reference, and the ground electrode was
730 placed on the right cheek. The electrooculogram (EOG) was recorded from above
731 and below the left eye and from the outer canthi of both eyes. EEG and EOG were
732 recorded with a band-pass filter of 0.01–100Hz, at a sampling rate of 1000Hz, which
733 was re-sampled to 500Hz offline. The impedance of all electrodes was kept below
734 10k Ω . EEG data were pre-analyzed using custom made routines in MatLab R2013b
735 (The Mathworks, Natick, MA, USA). EEG data were re-referenced off-line to the
736 average of all electrodes and filtered with a 0.5–30Hz pass-band. Epochs were
737 extracted stimulus-locked from -1500ms to 2500ms. Artefact-contaminated epochs
738 were excluded using the pop_autorej function in EEGLAB v13.0.1⁸⁶, which first
739 excludes trials with voltage fluctuations larger than 1000 μ V, and then excludes trials
740 with data values outside five standard deviations (mean=9.7% SE=2.9% of trials
741 removed). Subsequently, EOG artefacts were corrected by a procedure based on a
742 linear regression method (lms_regression function in MatLab R2013b)⁸⁷. Because
743 perceptually relevant, pre-stimulus alpha activity shows hemispheric lateralization,
744 relative to upcoming stimulus location, we recoded electrode positions as
745 contralateral versus ipsilateral to the hemifield of stimulus presentation (resulting in
746 all contralateral activity being on one side, which was conventionally defined to be
747 the right), i.e. for RVF-stimulus epochs, data from the contralateral (left) electrodes
748 were copied and flipped to right-sided electrodes, electrodes on the midline were not
749 flipped or recoded.

750 In order to identify the individual alpha-frequency peak during the task, data
751 epochs in the cue-stimulus period (i.e. pre-stimulus alpha from -1000ms to stimulus
752 presentations, baseline between -1500 and -1000ms) were analyzed with a fast
753 Fourier transformation (MatLab function spectopo, frequency resolution: 0.166Hz).
754 Power was calculated separately for each subject and condition and was normalized
755 by z-score decibel ($\text{dB}=10*\log_{10}[-\text{power}/\text{baseline}]$) transformation at each frequency.
756 Individual alpha-frequency was defined as the local maximum power within the
757 frequency range 7-13Hz (i.e. alpha peak). Each subject showed a clear peak within
758 this alpha range. However, a peak in the alpha-band was not present at all
759 electrodes. For this reason, power spectra on all parietal-occipital electrodes were
760 visually inspected. Then, the contralateral electrode was selected for analyses where
761 alpha oscillation showed a clear peak²³. Homologous electrodes were selected for
762 the analyses in the ipsilateral hemisphere. This procedure identified the following
763 subset of parieto-occipital electrodes that were used separately for each subject and
764 condition to identify alpha-frequency in the cue-stimulus period: contralateral
765 electrodes (P8,PO8,PO4,O2), and ipsilateral electrodes (P7,PO7,PO3,O1).
766 Importantly, most of the participants (n=15) showed maximum power over electrode
767 O2.

768 The amplitude of alpha oscillations was calculated by time-frequency analyses
769 of data epoched from 2000ms before to 2000ms after the stimulus onset. Long
770 epochs prevent edge artefacts from contaminating time frequency power in the time
771 windows of interest. Spectral EEG activity was assessed by time-frequency
772 decomposition using a complex sinusoidal wavelet convolution procedure (between
773 2 and 25 cycles per wavelet, linearly increasing across 50 linear-spaced frequencies
774 from 2.0Hz to 50.0Hz) with the newtimef function from EEGLAB v13.0.1⁸⁶ and

775 custom routines in MatLab. The resulting power was normalized by decibel
776 ($\text{dB}=10*\log_{10}[-\text{power}/\text{baseline}]$) transformation at each frequency, using a single trial
777 baseline between -1000 and -500 preceding stimulus onset. This long baseline
778 window was used to increase the signal-to-noise ratio during the baseline period and
779 is frequently applied in time frequency analyses^{88,89}. This procedure was applied
780 separately for each subject and condition. Mean alpha (7-13Hz) amplitude was
781 computed separately for each condition in the cue-stimulus interval (-500 to 0ms)¹⁸
782 and in the post-stimulus interval (0 to 900ms), which corresponds to the pre-
783 confidence prompt time period. In order to identify electrode clusters for the analyses
784 of alpha-amplitude, we used the same procedure as for alpha-frequency. For alpha-
785 amplitude, the following subsets of posterior contralateral (P2,P4,P8,PO4,PO8,O2)
786 and ipsilateral (P1,P3,P7,PO3,PO7,O1) electrodes were used for the analyses.
787 Importantly, as for alpha-frequency, most of the participants (n=18) showed
788 maximum alpha-amplitude over electrode O2.

789

790 *Statistical Analyses.* First, trials were sorted according to objective accuracy
791 (i.e. into correct and error trials). Correct trials consisted of correctly detected target
792 trials (i.e. hits, where participants pressed the spacebar after a target trial) and
793 correctly detected catch trials (i.e. correct rejections, where participants did not press
794 the spacebar after a catch trial). Accordingly, error trials consisted of misses after
795 target trials and false alarms after catch trials. Then we compared participants with
796 high vs low perceptual sensitivity. Perceptual sensitivity was estimated using the d'
797 measure. In signal detection theory (SDT²⁸), d' reflects standardized measure of
798 discrimination abilities between the signal and the noise (type I sensitivity). d' was
799 calculated as $d'=z(H) - z(\text{FA})$, where z represents the z-scores of Hit rate (i.e. H, the

800 probability of correct reactions on target trials) and false alarms (i.e. FA, the
801 probability of incorrect reactions on catch trials²⁸).

802 Next, we focused on subjective confidence levels during correct trials (i.e. hits
803 and correct rejections). In order to compare confident vs. non-confident responses,
804 we aggregated high confident responses and low confident responses. In this way,
805 correct trials were divided in high confident (i.e. with a confidence rating of 3 or 4) and
806 low confident (i.e. with a confidence rating of 1 or 2) trials. Then, we compared
807 participants showing high vs low confidence or metacognitive performance. For
808 confidence analyses, the mean value of the confidence ratings was calculated for
809 each participant. Instead, metacognitive performance was quantified using the
810 computational method proposed by Maniscalco & Lau²⁹. This method quantifies the
811 efficacy of confidence ratings to discriminate between correct and erroneous
812 responses in a SDT model. The model accounts for the variance in task performance
813 to compute metacognitive sensitivity (type II sensitivity) on subjective confidence
814 rating. This method, previously described in detail and validated, can give a metric
815 (termed *meta-d'*) for metacognitive abilities^{29,90}. Briefly, the central idea is to link type
816 I and type II SDT models to compute the observed type II sensitivity. *meta-d'*
817 estimates the values, which maximize the fit between the observed type II data and
818 the parameter values of the *d'* type I SDT model. Here, *meta-d'* was calculated with
819 the function `fit_meta_d_SSE` in MatLab. This function minimizes the sum of squared
820 errors and estimates *meta-d'* using observed type II data and the empirical type I
821 criterion *c'*⁹⁰. In this way, *meta-d'* estimates, for instance, the relative likelihood to
822 report a high confidence rating after a correct response^{29,90}. Higher values of *meta-d'*
823 correspond to participants having better metacognitive abilities.

824 Within participants EEG analyses were performed separately for objective
825 accuracy and subjective confidence. For *Objective Accuracy*, we compared alpha
826 activity (both frequency and amplitude) in 2x2 repeated measures ANOVAs with the
827 factors ACCURACY (correct and incorrect) and HEMISPHERE (contralateral and
828 ipsilateral). For Subjective Confidence, analyses were performed on correct trials⁶⁵.
829 Alpha activity was analyzed for the factor CONFIDENCE (high and low confidence)
830 and for the factor HEMISPHERES (contralateral and ipsilateral) in 2x2 repeated
831 measures ANOVAs. Differences between conditions were tested by one or two-tailed
832 t-tests (planned comparisons).

833 Between participants EEG analyses were performed on perceptual sensitivity
834 and metacognitive performance. For perceptual sensitivity analyses, we divided
835 participants in two numerically equivalent groups using the median split of the d'
836 scores (high vs low d'). As for perceptual sensitivity, we also conducted between-
837 group analysis, by dividing participants in two numerically equivalent groups (high vs
838 low meta d' scores) on a median split basis of the meta-d' scores (i.e. metacognitive
839 performance). Differences between groups were tested by one or two-tailed
840 independent samples t-tests (planned comparisons).

841

842 *Pre-stimulus IAF and resting-state IAF.* As we have used resting IAF to target
843 pre-stimulus activity in experiments 2 and 3 (see results sections), we checked for
844 any potential difference between resting-state IAF and pre-stimulus IAF in
845 Experiment 1 to ensure adequacy of our approach, with the working hypothesis that
846 no significant differences should be observed. In this analysis, resting-state IAF was
847 defined as the maximum local power in the alpha-frequency range during the resting
848 state over a cluster of posterior electrodes (O1,P1,P3,P5,P7,Pz,POz,Oz,PO3,PO7;

849 O2,P2,P4,P6,P8,PO4,PO8), while pre-stimulus IAF was calculated in the same
850 electrode cluster across conditions in a time window between -1000ms and stimulus
851 presentation. The analysis was performed on 22 out of 24 participants as resting
852 EEG was not available for 2 participants. As expected, the two-tailed paired samples
853 t-test showed no differences ($t(21)=0.05$, $p=.968$, $d=.019$) between resting state IAF
854 ($M=10.81\text{Hz}$; $SE=0.21\text{Hz}$) and pre-stimulus IAF ($M=10.83\text{Hz}$; $SE=0.37\text{Hz}$).
855 Importantly, these results demonstrate that resting-state IAF and pre-stimulus IAF
856 are comparable within group.

857

858 ***Experiment 2***

859 *EEG recordings –acquisition and processing.* EEG data were collected for
860 Experiment 2 as for Experiment 1. However, in Experiment 2, a rhythmic-TMS pulse
861 train was applied during EEG recording. The resulting rhythmic-TMS artefacts were
862 identified and removed using an open-source EEGLab extension, the TMS-EEG
863 signal analyzer (TESA)⁹¹. First, EEG data were epoched around stimulus onset
864 (between -1500ms and 2500ms for Experiment 2 and between -1000ms and
865 2000ms for Experiment 3, due to differences in stimulation timing) and the linear
866 trend from the obtained epochs was removed. Then rhythmic-TMS pulse artefact
867 and peaks of rhythmic-TMS-evoked scalp muscle activities were removed (-10ms
868 +10ms) and cubic interpolation was performed prior to down-sampling the data (from
869 5000Hz to 1000Hz). Interpolated data was again removed prior to Individual
870 Component Analysis (ICA). Specifically, a fastICA algorithm was used
871 (pop_tesa_fastica function: <http://research.ics.aalto.fi/ica/fastica/code/dlcode.shtml>)
872 to identify individual components representing artefacts, along with automatic
873 component classification (pop_tesa_compselect function), where each component

874 was subsequently manually checked and reclassified when necessary. In this first
875 round of ICA, only components with large amplitude artefacts, such as rhythmic-
876 TMS-evoked scalp muscle artefacts, were eliminated. Data were again interpolated
877 prior to applying pass-band (between 1 and 100Hz) and stop-band (between 48 and
878 52Hz) Butterworth filters. Subsequently interpolated data were again removed prior
879 to the second round of ICA, in order to remove all other artefacts, such as blinks, eye
880 movement, persistent muscle activity and electrode noise. Then, rhythmic-TMS-
881 pulse period was interpolated and data was re-referenced to the average of all
882 electrodes. Finally, single trials were visually inspected and those containing residual
883 rhythmic-TMS artefact were removed. The described rhythmic-TMS artefact removal
884 procedure was applied to all EEG data, both for active rhythmic-TMS and sham
885 stimulations. On average, approximately one third of all epochs were removed
886 ($M=34.31\%$, $SE=1.72\%$) (remaining epochs mean=236.5 epochs, $SE=6.19$). A
887 graphical explanation of the artefact correction procedure is reported in the
888 supplemental information (see supplemental figure S3).

889 Alpha-frequency and alpha-amplitude were identified in a similar manner as per
890 Experiment 1. Alpha-frequency was defined as the local maximum power within the
891 frequency 7-13Hz range in a pre-stimulus period (-650ms to stimulus presentation).
892 Accordingly, pre-stimulus alpha-amplitude was calculated in the time frequency data
893 (as for Experiment 1). The time window of analyses corresponded to stimulation
894 period for both alpha-frequency and -amplitude. Near-stimulation parieto-occipital
895 electrodes in the right hemisphere (PO4,PO8,O2), along with analogous electrodes
896 in the left hemisphere (PO3,PO7,O1) were used for all of the analyses.
897

898 *Statistical analyses (behavioral data).* Behavioral data were analyzed
899 separately for perceptual sensitivity (d' score) and for confidence (mean of
900 confidence ratings) and metacognitive performance (meta d' score).

901

902 All scores were compared between the two HEMIFIELDS (left and right) and
903 two STIMULATION types (active rhythmic-TMS and sham) in three GROUPs of
904 participants (IAF \pm 1Hz, IAF), in 2x2x3 repeated measures mixed-model ANOVAs.

905

906 *Statistical analyses (EEG data).* Electrophysiological data were analyzed
907 separately for pre-stimulus alpha-amplitude and alpha-frequency. Therefore, both
908 parameters of alpha activity were compared between the two HEMISPHERES (left
909 and right parieto-occipital cluster) and the two STIMULATION types (active rhythmic-
910 TMS and sham) in three GROUPs of participants in 2x2x3 repeated measures
911 mixed-model ANOVAs. Differences between conditions were tested by two-tailed t-
912 test (planned comparisons).

913 Finally, the association between rhythmic-TMS-evoked differences in alpha-
914 frequency in the stimulated (right) hemisphere (computed as a difference in alpha-
915 frequency between active rhythmic-TMS and sham stimulation conditions) and
916 differences in perceptual sensitivity in the opposite (left) hemispace (computed as a
917 difference in d' score between active rhythmic-TMS and sham stimulation conditions)
918 was explored via linear regression.

919

920 **Experiment 3**

921 *EEG recordings – acquisition and processing.* EEG data were recorded and
922 alpha-frequency and alpha-amplitude identified as in Experiments 1 and 2, with the

923 only difference being that the analysis window was moved to a time window
924 preceding the confidence prompt (850ms to 1500ms after stimulus presentation,
925 which corresponded to -650ms prior to the confidence prompt).

926

927 *Statistical analyses (behavioral data).* Behavioral data were analyzed
928 separately for perceptual sensitivity (d' score) and for confidence (mean of
929 confidence ratings) and metacognitive performance (meta d' score). All scores were
930 compared for the two HEMIFIELDS (left and right) and between different
931 STIMULATION types (active rhythmic-TMS and sham) in a 2x2 repeated measures
932 ANOVA.

933

934 *Statistical analyses (EEG data).* Electrophysiological data were analyzed
935 separately for alpha-amplitude and alpha-frequency. Moreover, differences in alpha-
936 amplitude and alpha-frequency were again compared between the two
937 HEMISPHERES (left and right) and between STIMULATION types (active rhythmic-
938 TMS and sham) in a 2x2 repeated measures ANOVA. Differences between
939 conditions were tested by two-tailed t-test (planned comparisons).

940 Finally, a linear regression model was used to determine whether rhythmic-
941 TMS-evoked differences in alpha-amplitude in the stimulated (right) hemisphere
942 (computed as a difference in alpha-amplitude between active rhythmic-TMS and
943 sham stimulation conditions) can predict differences in confidence levels in the
944 opposite (left) hemifield (computed as a difference in meta d' scores between active
945 rhythmic-TMS and sham stimulation conditions).

References

- 946 1. Hirst, W., Phelps, E.A., Meksin, R., Vaidya, C.J., Johnson, M.K., Mitchell, K.J.,
947 Buckner, R.L., Budson, A.E., Gabrieli, J.D.E., Lustig, C., et al. (2015). A ten-year follow-up
948 of a study of memory for the attack of September 11, 2001: Flashbulb memories and
949 memories for flashbulb events. *Journal of Experimental Psychology: General* *144*, 604–623.
- 950 2. Garry, M., Manning, C.G., Loftus, E.F., and Sherman, S.J. (1996). Imagination
951 inflation: Imagining a childhood event inflates confidence that it occurred. *Psychonomic*
952 *Bulletin and Review* *3*, 208–214.
- 953 3. Ferri, F., Venskus, A., Fotia, F., Cooke, J., and Romei, V. (2018). Higher proneness to
954 multisensory illusions is driven by reduced temporal sensitivity in people with high
955 schizotypal traits. *Consciousness and Cognition* *65*, 263–270.
- 956 4. Fenner, B., Cooper, N., Romei, V., and Hughes, G. (2020). Individual differences in
957 sensory integration predict differences in time perception and individual levels of schizotypy.
958 *Consciousness and Cognition* *84*, 102979.
- 959 5. Köther, U., Lincoln, T.M., and Moritz, S. (2018). Emotion perception and
960 overconfidence in errors under stress in psychosis. *Psychiatry Research* *270*, 981–991.
- 961 6. Klimesch, W., Sauseng, P., and Hanslmayr, S. (2007). EEG alpha oscillations: The
962 inhibition-timing hypothesis. *Brain Research Reviews* *53*, 63–88.
- 963 7. Mazaheri, A., and Jensen, O. (2010). Rhythmic pulsing: linking ongoing brain activity
964 with evoked responses. *Frontiers in Human Neuroscience* *4*, 1–13.
- 965 8. Palva, S., and Palva, J.M. (2007). New vistas for α -frequency band oscillations.
966 *Trends in Neurosciences* *30*, 150–158.
- 967 9. Samaha, J., Iemi, L., Haegens, S., and Busch, N.A. (2020). Spontaneous Brain
968 Oscillations and Perceptual Decision-Making. *Trends in Cognitive Sciences* *24*, 639–653.
- 969 10. Zazio, A., Schreiber, M., Miniussi, C., and Bortoletto, M. (2020). Modelling the
970 effects of ongoing alpha activity on visual perception: The oscillation-based probability of
971 response. *Neuroscience and Biobehavioral Reviews* *112*, 242–253.
- 972 11. Zoefel, B., and VanRullen, R. (2017). Oscillatory mechanisms of stimulus processing
973 and selection in the visual and auditory systems: State-of-the-art, speculations and
974 suggestions. *Frontiers in Neuroscience* *11*, 1–13.
- 975 12. VanRullen, R. (2016). Perceptual Cycles. *Trends in Cognitive Sciences* *20*, 723–735.
- 976 13. Wutz, A., and Melcher, D. (2014). The temporal window of individuation limits
977 visual capacity. *Frontiers in Psychology* *5*, 1–14.
- 978 14. Jensen, O., Gips, B., Bergmann, T.O., and Bonnefond, M. (2014). Temporal coding
979 organized by coupled alpha and gamma oscillations prioritize visual processing. *Trends in*
980 *Neurosciences* *37*, 357–369.
- 981 15. Busch, N.A., and VanRullen, R. (2010). Spontaneous EEG oscillations reveal periodic
982 sampling of visual attention. *Proceedings of the National Academy of Sciences* *107*, 16048–
983 16053.
- 984 16. Romei, V., Brodbeck, V., Michel, C., Amedi, A., Pascual-Leone, A., and Thut, G.
985 (2008). Spontaneous fluctuations in posterior α -band EEG activity reflect variability in
986 excitability of human visual areas. *Cerebral Cortex* *18*, 2010–2018.
- 987 17. Benwell, C.S.Y., Tagliabue, C.F., Veniero, D., Cecere, R., Savazzi, S., and Thut, G.
988 (2017). Pre-stimulus EEG power predicts conscious awareness but not objective visual
989 performance. *Eneuro* *4*, ENEURO.0182-17.2017.
- 990 18. Samaha, J., Iemi, L., and Postle, B.R. (2017). Prestimulus alpha-band power biases
991 visual discrimination confidence, but not accuracy. *Consciousness and Cognition* *54*, 47–55.
- 992 19. Iemi, X.L., Chaumon, M., Se, X., Crouzet, M., and Busch, X.N.A. (2017).
993 Spontaneous Neural Oscillations Bias Perception by Modulating Baseline Excitability.

- 994 Journal of Neuroscience 37, 807–819.
- 995 20. Limbach, K., and Corballis, P.M. (2016). Prestimulus alpha power influences
996 response criterion in a detection task. *Psychophysiology* 53, 1154–1164.
- 997 21. Cecere, R., Rees, G., and Romei, V. (2015). Individual differences in alpha frequency
998 drive crossmodal illusory perception. *Current Biology* 25, 231–235.
- 999 22. Minami, S., and Amano, K. (2017). Illusory Jitter Perceived at the Frequency of
1000 Alpha Oscillations. *Current Biology* 27, 2344–2351.
- 1001 23. Samaha, J., and Postle, B.R. (2015). The Speed of Alpha-Band Oscillations Predicts
1002 the Temporal Resolution of Visual Perception. *Current Biology* 25, 2985–2990.
- 1003 24. Wutz, A., Melcher, D., and Samaha, J. (2018). Frequency modulation of neural
1004 oscillations according to visual task demands. *Proceedings of the National Academy of
1005 Sciences of the United States of America* 115, 1346–1351.
- 1006 25. Cooke, J., Poch, C., Gillmeister, H., Costantini, M., and Romei, V. (2019). Oscillatory
1007 Properties of Functional Connections Between Sensory Areas Mediate Cross-Modal Illusory
1008 Perception. *The Journal of neuroscience : the official journal of the Society for Neuroscience*
1009 39, 5711–5718.
- 1010 26. Migliorati, D., Zappasodi, F., Perrucci, M.G., Donno, B., Northoff, G., Romei, V.,
1011 and Costantini, M. (2020). Individual Alpha Frequency Predicts Perceived Visuotactile
1012 Simultaneity. *Journal of Cognitive Neuroscience* 32, 1–11.
- 1013 27. Mierau, A., Klimesch, W., and Lefebvre, J. (2017). State-dependent alpha peak
1014 frequency shifts: Experimental evidence, potential mechanisms and functional implications.
1015 *Neuroscience*.
- 1016 28. Green, D.M., and Swets, J.A. (1966). *Signal detection theory and psychophysics*. John
1017 Wiley, ed. (Oxford, England).
- 1018 29. Maniscalco, B., and Lau, H. (2012). A signal detection theoretic approach for
1019 estimating metacognitive sensitivity from confidence ratings. *Consciousness and Cognition*.
- 1020 30. Yeung, N., and Summerfield, C. (2012). Metacognition in human decision-making:
1021 confidence and error monitoring. *Philosophical Transactions of the Royal Society B:
1022 Biological Sciences* 367, 1310–1321.
- 1023 31. Murphy, P.R., Robertson, I.H., Harty, S., and O’Connell, R.G. (2015). Neural
1024 evidence accumulation persists after choice to inform metacognitive judgments. *eLife*, 1–23.
- 1025 32. Pleskac, T.J., and Busemeyer, J.R. (2010). Two-stage dynamic signal detection: A
1026 theory of choice, decision time, and confidence. *Psychological Review* 117, 864–901.
- 1027 33. Iemi, L., Busch, N.A., Laudini, A., Haegens, S., Samaha, J., Villringer, A., and
1028 Nikulin, V. V. (2019). Multiple mechanisms link prestimulus neural oscillations to sensory
1029 responses. *eLife* 8, 1–34.
- 1030 34. Romei, V., Thut, G., Mok, R.M., Schyns, P.G., and Driver, J. (2012). Causal
1031 implication by rhythmic transcranial magnetic stimulation of alpha frequency in feature-
1032 based local vs. global attention. *The European journal of neuroscience* 35, 968–974.
- 1033 35. Romei, V., Driver, J., Schyns, P.G., and Thut, G. (2011). Rhythmic TMS over Parietal
1034 Cortex Links Distinct Brain Frequencies to Global versus Local Visual Processing. *Current
1035 Biology* 21, 334–337.
- 1036 36. Romei, V., Thut, G., and Silvanto, J. (2016). Information-Based Approaches of
1037 Noninvasive Transcranial Brain Stimulation. *Trends in Neurosciences* 39, 782–795.
- 1038 37. Thut, G., Veniero, D., Romei, V., Miniussi, C., Schyns, P., and Gross, J. (2011).
1039 Rhythmic TMS causes local entrainment of natural oscillatory signatures. *Current Biology*
1040 21, 1176–1185.
- 1041 38. Helfrich, R.F., Schneider, T.R., Rach, S., Trautmann-Lengsfeld, S.A., Engel, A.K.,
1042 and Herrmann, C.S. (2014). Entrainment of brain oscillations by transcranial alternating
1043 current stimulation. *Current Biology* 24, 333–339.

- 1044 39. Thut, G., Bergmann, T.O., Fröhlich, F., Soekadar, S.R., Brittain, J.S., Valero-Cabré,
1045 A., Sack, A.T., Miniussi, C., Antal, A., Siebner, H.R., et al. (2017). Guiding transcranial
1046 brain stimulation by EEG/MEG to interact with ongoing brain activity and associated
1047 functions: A position paper. *Clinical Neurophysiology* 128, 843–857.
- 1048 40. Veniero, D., Vossen, A., Gross, J., and Thut, G. (2015). Lasting EEG/MEG
1049 aftereffects of rhythmic transcranial brain stimulation: Level of control over oscillatory
1050 network activity. *Frontiers in Cellular Neuroscience* 9, 1–17.
- 1051 41. Romei, V., Bauer, M., Brooks, J.L., Economides, M., Penny, W., Thut, G., Driver, J.,
1052 and Bestmann, S. (2016). Causal evidence that intrinsic beta-frequency is relevant for
1053 enhanced signal propagation in the motor system as shown through rhythmic TMS.
1054 *NeuroImage* 126, 120–130.
- 1055 42. Ergenoglu, T., Demiralp, T., Bayraktaroglu, Z., Ergen, M., Beydagi, H., and Uresin,
1056 Y. (2004). Alpha rhythm of the EEG modulates visual detection performance in humans.
1057 *Cognitive Brain Research* 20, 376–383.
- 1058 43. van Dijk, H., Schoffelen, J.-M., Oostenveld, R., and Jensen, O. (2008). Prestimulus
1059 Oscillatory Activity in the Alpha Band Predicts Visual Discrimination Ability. *Journal of*
1060 *Neuroscience* 28, 1816–1823.
- 1061 44. Roberts, D.M., Fedota, J.R., Buzzell, G.A., Parasuraman, R., and McDonald, C.G.
1062 (2014). Prestimulus Oscillations in the Alpha Band of the EEG Are Modulated by the
1063 Difficulty of Feature Discrimination and Predict Activation of a Sensory Discrimination
1064 Process. *Journal of Cognitive Neuroscience* 26, 1615–1628.
- 1065 45. Baumgarten, T.J., Schnitzler, A., and Lange, J. (2016). Prestimulus Alpha Power
1066 Influences Tactile Temporal Perceptual Discrimination and Confidence in Decisions.
1067 *Cerebral Cortex* 26, 891–903.
- 1068 46. Iemi, L., and Busch, N.A. (2018). Moment-to-Moment Fluctuations in Neuronal
1069 Excitability Bias Subjective Perception Rather than Strategic Decision-Making. *Eneuro* 5, 1–
1070 13.
- 1071 47. Weisz, N., Lüchinger, C., Thut, G., and Müller, N. (2014). Effects of individual alpha
1072 rTMS applied to the auditory cortex and its implications for the treatment of chronic tinnitus.
1073 *Hum Brain Mapp* 35, 14–29.
- 1074 48. Hanslmayr, S., Matuschek, J., and Fellner, M.-C. (2014). Entrainment of prefrontal
1075 beta oscillations induces an endogenous echo and impairs memory formation. *Curr Biol* 24,
1076 904–909.
- 1077 49. Varela, F.J., Toro, A., Roy John, E., and Schwartz, E.L. (1981). Perceptual framing
1078 and cortical alpha rhythm. *Neuropsychologia* 19, 675–686.
- 1079 50. Mathewson, K.E., Gratton, G., Fabiani, M., Beck, D.M., and Ro, T. (2009). To See or
1080 Not to See: Prestimulus Phase Predicts Visual Awareness. *Journal of Neuroscience* 29, 2725–
1081 2732.
- 1082 51. Dugué, L., Marque, P., and VanRullen, R. (2011). The phase of ongoing oscillations
1083 mediates the causal relation between brain excitation and visual perception. *Journal of*
1084 *Neuroscience* 31, 11889–11893.
- 1085 52. Busch, N.A., Dubois, J., and VanRullen, R. (2009). The phase of ongoing EEG
1086 oscillations predicts visual perception. *Journal of Neuroscience* 29, 7869–7876.
- 1087 53. Haegens, S., Nacher, V., Luna, R., Romo, R., and Jensen, O. (2011). α -Oscillations in
1088 the monkey sensorimotor network influence discrimination performance by rhythmical
1089 inhibition of neuronal spiking. *PNAS* 108, 19377–19382.
- 1090 54. Navajas, J., Bahrami, B., and Latham, P.E. (2016). Post-decisional accounts of biases
1091 in confidence. *Current Opinion in Behavioral Sciences* 11, 55–60.
- 1092 55. Fleming, S.M., and Daw, N.D. (2017). Self-Evaluation of Decision-Making: A
1093 General Bayesian Framework for Metacognitive Computation. *Psychol Rev* 124, 91–114.

- 1094 56. Pereira, M., Faivre, N., Iturrate, I., Wirthlin, M., Serafini, L., Martin, S., Desvachez,
1095 A., Blanke, O., Van De Ville, D., and Millán, J. del R. (2020). Disentangling the origins of
1096 confidence in speeded perceptual judgments through multimodal imaging. *Proc Natl Acad*
1097 *Sci USA* *117*, 8382–8390.
- 1098 57. Posner, M.I., Snyder, C.R., and Davidson, B.J. (1980). Attention and the detection of
1099 signals. *Journal of Experimental Psychology: General* *109*, 160–174.
- 1100 58. Fan, J., McCandliss, B.D., Sommer, T., Raz, A., and Posner, M.I. (2002). Testing the
1101 Efficiency and Independence of Attentional Networks. *Journal of Cognitive Neuroscience* *14*,
1102 340–347.
- 1103 59. Thut, G., Nietzel, A., Brandt, S., and Pascual-Leone, A. (2006). Alpha Band
1104 Electroencephalographic Activity over Occipital Cortex Indexes Visuospatial Attention Bias
1105 and Predicts Visual Target Detection. *Journal of Neuroscience* *13*, 9494–9502.
- 1106 60. Rihs, T.A., Michel, C.M., and Thut, G. (2007). Mechanisms of selective inhibition in
1107 visual spatial attention are indexed by α -band EEG synchronization. *European Journal of*
1108 *Neuroscience* *25*, 603–610.
- 1109 61. Tarasi, L., Trajkovic, J., Diciotti, S., di Pellegrino, G., Ferri, F., Ursino, M., and
1110 Romei, V. (2021). Predictive waves in the autism-schizophrenia continuum: A novel
1111 biobehavioral model. *Neurosci Biobehav Rev* *132*, 1–22.
- 1112 62. Haegens, S., Cousijn, H., Wallis, G., Harrison, P.J., and Nobre, A.C. (2014). Inter-
1113 and intra-individual variability in alpha peak frequency. *NeuroImage*.
- 1114 63. Hülzdünker, T., Mierau, A., and Strüder, H.K. (2016). Higher balance task demands
1115 are associated with an increase in individual alpha peak frequency. *Frontiers in Human*
1116 *Neuroscience*.
- 1117 64. Maurer, U., Brem, S., Liechti, M., Maurizio, S., Michels, L., and Brandeis, D. (2014).
1118 Frontal Midline Theta Reflects Individual Task Performance in a Working Memory Task.
1119 *Brain Topography*.
- 1120 65. Samaha, J., Bauer, P., Cimaroli, S., and Postle, B.R. (2015). Top-down control of the
1121 phase of alpha-band oscillations as a mechanism for temporal prediction. *Proceedings of the*
1122 *National Academy of Sciences of the United States of America* *112*, 8439–8444.
- 1123 66. Benwell, C.S.Y., Coldea, A., Harvey, M., and Thut, G. (2021). Low pre-stimulus
1124 EEG alpha power amplifies visual awareness but not visual sensitivity. *European Journal of*
1125 *Neuroscience*, 1–16.
- 1126 67. Romei, V., Gross, J., and Thut, G. (2010). On the role of prestimulus alpha rhythms
1127 over occipito-parietal areas in visual input regulation: Correlation or causation? *Journal of*
1128 *Neuroscience* *30*, 8692–8697.
- 1129 68. Albouy, P., Weiss, A., Baillet, S., and Zatorre, R.J. (2017). Selective Entrainment of
1130 Theta Oscillations in the Dorsal Stream Causally Enhances Auditory Working Memory
1131 Performance. *Neuron* *94*, 193-206.e5.
- 1132 69. Vernet, M., Stengel, C., Quentin, R., Amengual, J.L., and Valero-Cabré, A. (2019).
1133 Entrainment of local synchrony reveals a causal role for high-beta right frontal oscillations in
1134 human visual consciousness. *Scientific Reports* *9*, 1–15.
- 1135 70. Sauseng, P., Klimesch, W., Heise, K.F., Gruber, W.R., Holz, E., Karim, A.A.,
1136 Glennon, M., Gerloff, C., Birbaumer, N., and Hummel, F.C. (2009). Brain Oscillatory
1137 Substrates of Visual Short-Term Memory Capacity. *Current Biology* *19*, 1846–1852.
- 1138 71. Chanes, L., Quentin, R., Tallon-Baudry, C., and Valero-Cabré, A. (2013). Causal
1139 frequency-specific contributions of frontal spatiotemporal patterns induced by non-invasive
1140 neurostimulation to human visual performance. *Journal of Neuroscience* *33*, 5000–5005.
- 1141 72. De Martino, B., Fleming, S.M., Garrett, N., and Dolan, R.J. (2013). Confidence in
1142 value-based choice. *Nature neuroscience* *16*, 105–10.
- 1143 73. Wolinski, N., Cooper, N.R., Sauseng, P., and Romei, V. (2018). The speed of parietal

1144 theta frequency drives visuospatial working memory capacity. *PLoS Biology*.

1145 74. Bestmann, S., Ruff, C.C., Blakemore, C., Driver, J., and Thilo, K. V (2007). Spatial
1146 Attention Changes Excitability of Human Visual Cortex to Direct Stimulation. *Current*
1147 *Biology* *17*, 134–139.

1148 75. Cattaneo, Z., Silvanto, J., Battelli, L., and Pascual-Leone, A. (2009). The mental
1149 number line modulates visual cortical excitability. *Neurosci Lett* *462*, 253–256.

1150 76. Silvanto, J., and Muggleton, N.G. (2008). A novel approach for enhancing the
1151 functional specificity of TMS: Revealing the properties of distinct neural populations within
1152 the stimulated region. *Clinical Neurophysiology* *119*, 124.

1153 77. Mevorach, C., Humphreys, G.W., and Shalev, L. (2006). Opposite biases in salience-
1154 based selection for the left and right posterior parietal cortex. *Nature Neuroscience*.

1155 78. Pitcher, D., Walsh, V., Yovel, G., and Duchaine, B. (2007). TMS Evidence for the
1156 Involvement of the Right Occipital Face Area in Early Face Processing. *Current Biology* *17*,
1157 1568–1573.

1158 79. Silvanto, J., Lavie, N., and Walsh, V. (2005). Double dissociation of V1 and V5/MT
1159 activity in visual awareness. *Cerebral Cortex* *15*, 1736–1741.

1160 80. Bolognini, N., Senna, I., Maravita, A., Pascual-Leone, A., and Merabet, L.B. (2010).
1161 Auditory enhancement of visual phosphene perception: The effect of temporal and spatial
1162 factors and of stimulus intensity. *Neuroscience Letters*.

1163 81. Gerwig, M., Kastrup, O., Meyer, B.U., and Niehaus, L. (2003). Evaluation of cortical
1164 excitability by motor and phosphene thresholds in transcranial magnetic stimulation. *Journal*
1165 *of the Neurological Sciences*.

1166 82. Romei, V., Murray, M.M., Cappe, C., and Thut, G. (2009). Preperceptual and
1167 Stimulus-Selective Enhancement of Low-Level Human Visual Cortex Excitability by
1168 Sounds. *Current Biology* *19*, 1799–1805.

1169 83. Romei, V., Murray, M.M., Merabet, L.B., and Thut, G. (2007). Occipital transcranial
1170 magnetic stimulation has opposing effects on visual and auditory stimulus detection:
1171 Implications for multisensory interactions. *Journal of Neuroscience* *27*, 11465–11472.

1172 84. Romei, V., Rihs, T., Brodbeck, V., and Thut, G. (2008). Resting
1173 electroencephalogram alpha-power over posterior sites indexes baseline visual cortex
1174 excitability. *NeuroReport* *19*, 203–208.

1175 85. Rossi, S., Hallett, M., Rossini, P.M., and Pascual-Leone, A. (2009). Safety, ethical
1176 considerations, and application guidelines for the use of transcranial magnetic stimulation in
1177 clinical practice and research. *Clin Neurophysiol* *120*, 2008–2039.

1178 86. Delorme, A., and Makeig, S. (2004). EEGLAB: An open source toolbox for analysis
1179 of single-trial EEG dynamics including independent component analysis. *Journal of*
1180 *Neuroscience Methods*.

1181 87. Gratton, G., Coles, M.G.H., and Donchin, E. (1983). A new method for off-line
1182 removal of ocular artifact. *Electroencephalography and Clinical Neurophysiology* *55*, 468–
1183 484.

1184 88. Cavanagh, J.F., Figueroa, C.M., Cohen, M.X., and Frank, M.J. (2012). Frontal theta
1185 reflects uncertainty and unexpectedness during exploration and exploitation. *Cerebral Cortex*
1186 *22*, 2575–2586.

1187 89. Di Gregorio, F., Maier, M.E., and Steinhauser, M. (2018). Errors can elicit an error
1188 positivity in the absence of an error negativity: Evidence for independent systems of human
1189 error monitoring. *NeuroImage* *172*, 427–436.

1190 90. Barrett, A.B., Dienes, Z., and Seth, A.K. (2013). Measures of metacognition on
1191 signal-detection theoretic models. *Psychological Methods* *18*, 535–552.

1192 91. Rogasch, N.C., Sullivan, C., Thomson, R.H., Rose, N.S., Bailey, N.W., Fitzgerald,
1193 P.B., Farzan, F., and Hernandez-Pavon, J.C. (2017). Analysing concurrent transcranial

1194 magnetic stimulation and electroencephalographic data: A review and introduction to the
1195 open-source TESA software. NeuroImage.
1196